UFBA

UNIVERSIDADE FEDERAL DA BAHIA

ESCOLA POLITÉCNICA

PROGRAMA DE PÓS GRADUAÇÃO EM ENGENHARIA INDUSTRIAL - PEI

DOUTORADO EM ENGENHARIA INDUSTRIAL

LUIS ALBERTO PARGAS CARMONA

PROCEDURE FOR EQUIPMENT SELECTION IN MECHANICAL SYSTEMS BASED ON CAPITAL COST MINIMIZATION AND OPTIMAL LOADING

PEI

Programa de Pós-Graduação em Engenharia Industrial

SALVADOR

2023

FEDERAL UNIVERSITY OF BAHIA
POLYTECHNIC SCHOOL
INDUSTRIAL ENGINEERING GRADUATE PROGRAM - PEI

LUIS ALBERTO PARGAS CARMONA

PROCEDURE FOR EQUIPMENT SELECTION IN MECHANICAL SYSTEMS BASED ON CAPITAL COST MINIMIZATION AND OPTIMAL LOADING

Salvador
2023

Ficha catalográfica elaborada pelo Sistema Universitário de Bibliotecas (SIBI/UFBA),
com os dados fornecidos pelo(a) autor(a).

Pargas Carmona, Luis Alberto
Procedure for equipment selection in mechanical systems based on capital cost minimization and optimal loading / Luis Alberto Pargas Carmona. -- Salvador, 2023.
93 f. : il

Orientador: Júlio Augusto Mendes da Silva.
Coorientador: Ângelo Márcio Oliveira Sant'Anna.
Tese (Doutorado - Programa de Pós-Graduação em Engenharia Industrial) -- Universidade Federal da Bahia, Escola Politécnica, 2023.

1. Chilled water systems. 2. FPSO. 3. Multi-objective optimization. 4. Optimal equipment selection. 5. Optimal loading problem. I. Mendes da Silva, Júlio Augusto. II. Oliveira Sant'Anna, Ângelo Márcio. III. Título.

LUIS ALBERTO PARGAS CARMONA

PROCEDURE FOR EQUIPMENT SELECTION IN MECHANICAL SYSTEMS BASED ON CAPITAL COST MINIMIZATION AND OPTIMAL LOADING

This thesis has been submitted in fulfilment of the requirements for the Doctor's Degree in Industrial Engineering at Federal University of Bahia.
Supervisor: Prof. Dr. Júlio Augusto Mendes da Silva
Co-supervisor: Prof. Dr. Ângelo Márcio Oliveira Sant'Anna

Salvador
2023

“PROCEDURE FOR EQUIPMENT SELECTION IN MECHANICAL SYSTEMS BASED ON CAPITAL COST MINIMIZATION AND OPTIMAL LOADING”.

LUIS ALBERTO PARGAS CARMONA

Tese submetida ao corpo docente do programa de pós-graduação em Engenharia Industrial da Universidade Federal da Bahia como parte dos requisitos necessários para a obtenção do grau de doutor em Engenharia Industrial.

Examinada por:

Prof. Dr. Júlio Augusto Mendes da Silva _____
Doutor em Engenharia Mecânica, pela Universidade de São Paulo, Brasil, 2013.
(Orientador PEI-UFBA)

Prof. Dr. Ângelo Márcio Oliveira Sant’Anna _____
Doutor em Engenharia de Produção, pela Universidade Federal do Rio Grande do Sul, Brasil, 2009.
(Coorientador PEI-UFBA)

Prof. Dr. Cristiano Hora de Oliveira Fontes _____
Doutor em Engenharia Química, pela Universidade Estadual de Campinas, Brasil, 2001.
(Membro Interno PEI-UFBA)

Prof. Dr. Lourenço Gobira Alves _____
Doutor em Engenharia Mecânica, pela Universidade Estadual de Campinas, Brasil, 2007.
(Membro Externo DEM-UFBA)

Prof. Dr. Cyro Albuquerque Neto _____
Doutor em Engenharia Mecânica, pela Universidade de São Paulo, Brasil, 2010.
(Membro Externo PPGEM-FEI)

Prof. Dr. Gilberto Reynoso Meza _____
Doutor em Automática, Robótica e Informática Industrial, pela Universitat Politècnica de València, Espanha, 2014.
(Membro Externo PPGEPS-PUCPR)

Salvador, BA - BRASIL
Agosto/2023

"If the system exhibits a structure which can be represented by a mathematical equivalent, called a mathematical model, and if the objective can be also so quantified, then some computational method may be evolved for choosing the best schedule of actions among alternatives."

George Dantzig

Acknowledgements

First of all, I would like to thank my supervisors Júlio Augusto Mendes da Silva and Ângelo Márcio Oliveira Sant'Anna for their constant support, patience and guidance at every stage of this research. I truly appreciate the time and effort you put into it.

I also want to express my gratitude to José Luis Risco Martín for his valuable insights and for being a generous host at the Complutense University of Madrid.

Special thanks to Cyro Albuquerque Neto, Daniel Alexander Flórez Orrego and Silvio de Oliveira Junior for their contribution to the second article derived from this thesis.

I am absolutely indebted with my family for their unconditional support and the time I took away from them.

This work was supported by the Coordination of Superior Level Staff Improvement – Brazil (CAPES) – Finance Code 001.

Abstract

Providing maximum performance at minimum cost is a major challenge in the design of mechanical systems. One of the key problems is determining the optimal schedule of a set of units operating in parallel (such as chillers or turbines) that minimizes the overall energy consumption. This is a widely studied problem in the literature known as "economic dispatch" (in power systems) or as "optimal loading problem" (in air-conditioning systems). However, the loading problem requires the units to be previously selected. This work proposes a procedure to solve the selection problem and the loading problem at the same time. The proposal is a novel procedure that allows determining, in a rigorous manner, the units that have to be purchased and the corresponding operation schedule. It was applied to two case studies: i) selection of chillers in cooling plants, and ii) selection of the utility plant in oil and gas offshore platforms. Both cases are analyzed using two alternative optimization approaches. First, a mono-objective optimization of a single cost-based function and, second, a multi-objective optimization of capital cost and energy consumption. The results in all cases showed that the total nominal capacity of the selected units is not necessarily closed to the peak load, which is a common rule-of-thumb guideline for equipment selection. In the case of the cooling plant, the nominal capacity of the chillers selected was up to 1.6 times the peak load demand. Likewise, the best solutions in the case of the utility plant consisted of very different-sized models. These counter-intuitive results demonstrate the importance of using a systematic selection procedure.
Keywords: Chilled water systems, FPSO, Mono-objective optimization, Multi-objective optimization, Optimal equipment selection, Optimal loading problem.

Resumo

Proporcionar o máximo desempenho com o custo mínimo é um desafio importante no desenho de instalações mecânicas. Um dos principais problemas é determinar a configuração ótima de um conjunto de unidades funcionando em paralelo (como chillers ou turbinas) que minimize o consumo total de energia. Este problema é amplamente estudado na literatura e é conhecido como "despacho econômico" (em sistemas de geração de potência) ou como "problema da carga ótima" (em sistemas de climatização). No entanto, este problema precisa que as unidades sejam selecionadas previamente. O procedimento proposto neste trabalho objetiva resolver o problema da seleção e o problema da carga simultaneamente. Esta é uma proposta que permite determinar, de maneira rigorosa, as unidades que devem ser compradas e a correspondente configuração de operação. O procedimento foi aplicado a dois estudos de caso: i) seleção de chillers em sistemas de água gelada, e ii) seleção de turbinas a gas e motores em plataformas offshore de petróleo e gas. Ambos os casos foram analisados utilizando duas abordagens alternativas. Em primeiro lugar, uma otimização monobjetivo de uma função combinada baseada no custo e, em segundo lugar, uma otimização multiobjetivo do custo de capital e do consumo de energia. Os resultados em todos os casos mostraram que a capacidade nominal total das unidades selecionadas não é necessariamente próxima da carga pico, que é uma regra geral habitualmente utilizada na seleção de equipamentos. No caso do sistema de água gelada, a capacidade nominal total dos chillers selecionados alcançou até 1.6 vezes a demanda máxima requerida. No caso da planta de utilidades na plataforma FPSO, as melhores soluções consistiram na seleção de equipamentos de diferente porte. Estes resultados contraintuitivos demonstram a necessidade da utilização de um procedimento sistemático de seleção.

Palavras-chave: FPSO, Otimização monobjetivo, Otimização multiobjetivo, Problema da carga ótima, Seleção ótima de equipamentos, Sistemas de água gelada.

List of Figures

List of Tables

Nomenclature

Subscripts

i = Unit model

j = Level of demand

k = Unit in the system

Decision variables

P_{ij} = Power status variable (On: $P_{ij} = 1$ / Off: $P_{ij} = 0$)

R_{ij} = Partial load ratio of unit i at level j

S_i = Selection variable

Parameters

α_{1i}, α_{2i},... = Capacity function regression parameters of model i

β_{0i}, β_{1i}, β_{2i},... = Consumption (or performance) function regression parameters of model i

C = Number of models available

c_i = Capital cost of unit i

d_j = Load demand at level j

G = Number of generations

m_i = Lower partial load limit of unit i

N = Number of units in the system

P = Number of levels of demand

q_i = Nominal capacity of unit i

r = Interest rate

T_j = Outdoor temperature at level j

t_j = Time at level j

w_1 = Energy price

w_2 = Depreciation rate

Other symbols

ϕ_{ij} = Capacity of unit i at level j when $P_{ij} = 1$

ψ_{ij} = Energy consumption of unit i at level j when $P_{ij} = 1$

g_{ij} = Actual consumption of unit i at level j

h_{ij} = Actual capacity of unit i at level j

I_H = Hypervolume indicator

v = Volume enclosed by a solution

W = Set of solutions

Acronyms

COP = Coefficient of performance

FPSO = Floating, production, storage and offloading

PLR = Partial load ratio

Contents

Chapter 1

Introduction

Selecting equipments in mechanical systems is not an easy task, especially in an increasingly competitive market with a wide variety of manufacturers, models and technologies available. An appropriate selection is one that meets the load demand with low energy consumption and an affordable cost. Another aspect that has to be taken into consideration in the equipment selection is the demand profile of the system. Analyzing the load fluctuation during the system lifetime is critical for making decisions based on the whole load profile instead of the peak load, which is normally an atypical condition. Decisions based on exclusively the peak load do not take advantage of variable-capacity units that operate more efficiently at partial load.

Once both the performance functions of the units (such as chillers or turbines) and the demand profile are estimated, it is possible to formulate an optimization problem whose objective is minimizing the overall energy consumption of the units operating in the system while meeting the demand constraints. This optimization problem is known as "economic dispatch" (in power systems) or as "optimal loading problem" (in air-conditioning systems). Addressing this problem requires the units to be previously selected. However, the selection of the units in the system usually dismisses the load profile and it is based upon arbitrary criteria such as dividing the peak load by a certain number of identical units.

The procedure proposed in this work integrates the optimal selection problem with the optimal loading problem. Solving these problems simultaneously is a novelty in the field of mechanical systems. It is evident that selecting the units from a set of models at disposal instead of having the units previously selected, increases the complexity of the problem, but this is a relatively minor issue considering the potential reduction in energy consumption and capital cost. In practical terms, a single formulation allows to determine the most suitable schedule for the best selection possible given the models available in the market.

There are a few rules of thumb for equipment selection in heating, ventilation and air-conditioning (HVAC) systems. For instance, it is a common practice to distribute the peak load evenly into the chillers in a cooling plant. Another usual strategy is breaking the load

profile down into time-based discrete groups to which the chillers are arbitrarily assigned. In both cases, the possibility of having a total installed capacity greater than the peak load is ignored because chiller redundancy is only considered when there is an actual need for high reliability. The chiller selection remains in the domain of engineering judgement and there is no formal procedure for selecting chillers in cooling plants. Nevertheless, there is a vast literature on the optimal chiller loading problem. Most of the authors approach this problem using bio-inspired algorithms, such as: improved invasive weed optimization (ZHENG; LI, 2018), improved artificial fish swarm algorithm (ZHENG; LI; DUAN, 2019), improved grasshopper optimization algorithm (WENHAN et al., 2019), quantum emperor penguin optimization algorithm (MIN; TANG; ROUYENDEGH, 2020), improved particle swarm optimization (TIAN et al., 2019b) and camel traveling behavior algorithm (CHEN et al., 2020).

Similarly, there is a gap in the state of the art in equipment selection for utility plants in floating, production, storage and offloading (FPSO) platforms. Flórez-Orrego et al. (2021) introduced a systematic framework to determine the most appropriate operating conditions and load distribution of a group of power units. In order to include the capital cost and the financial feasibility in the analysis, Flórez-Orrego et al. (2022) performed a techno-economic assessment to determine the optimal configuration of centralized power stations designed for supplying the electricity required by various identical FPSO. However, apart from a few exceptions, such as the works of Koch, Cziesla & Tsatsaronis (2007) and Cao et al. (2017), most of the literature focused on minimizing the total power consumption of an arrangement of units that have been previously selected. The most preferred optimization techniques in this field are genetic algorithms considering energy, economic and environmental variables. Some examples are offered by Mohagheghi & Shayegan (2009), Ahmadi, Dincer & Rosen (2011), Ahmadi & Dincer (2011a), Ahmadi & Dincer (2011b), Rovira et al. (2011), Sayyaadi & Mehrabipour (2012), Shamoushaki Farrokh Ghanatir & Ahmadi (2017) and Rezaie, Tsatsaronis & Hellwig (2019). It is also a common practice to combine different approaches. For instance, in Allahyarzadeh-Bidgoli et al. (2021) both non-dominated sorting genetic algorithm II (NSGA-II) and a gradient-based method were used to minimize the total power consumption in a FPSO platform.

1.1 Justification

Energy efficiency is a major concern in the design of HVAC systems because they normally demand more energy than any other system in commercial and office buildings. According to Thangavelu, Myat & Khambadkone (2017) the cooling load accounts for 45-60% of the total energy consumption. In a similar manner, the development of solutions for reducing energy consumption and CO2-emissions in offshore plants has gained increasing

interest in recent years. Some solutions are assessed by Nguyen et al. (2016). In both cases, equipment selection plays a major role in reducing the energy consumption. Even a system operating at its optimal loading is restricted to the performance of the units selected.

Two main strategies have been commonly used for equipment selection in the design of mechanical systems. The first strategy consists in distributing the peak load evenly over a number of units determined by experience. On the other hand, the second strategy consists in sizing each unit according to a discretionary distribution of the load profile and the corresponding operating time at each level of demand. Certainly, this strategy acknowledges that the peak load may be demanded only during a tiny fraction of the operating time and, therefore, any decision on the selection of the units should be taken after a careful analysis of the load profile, but it is also based upon arbitrary criteria.

The selection problem is not tackled very differently even by sophisticated engineers. In contrast, there is a vast literature on the optimal loading problem and the use of multiple algorithms to solve it. Determining the load share of the units at each level of demand is critical to design appropriate control strategies in existing systems, but solving this problem does not provide any insight on the models that have to be purchased. The selection problem has been overlooked in academic papers as well as in technical papers and guidelines. The selection procedure presented here is a novelty that constitutes a solid starting point for further research on the topic.

1.2 Objectives

1.2.1 General objective

Develop a procedure to solve the selection problem and the loading problem simultaneously.

1.2.2 Specific objectives

- Apply the developed procedure to the problem of selecting chillers in chilled water systems.
- Apply the developed procedure to the problem of selecting the utility plant in oil and gas offshore platforms.
- Compare the results of the mono-objective and multi-objective approaches in the cases analyzed.

1.3 Contributions and ineditism

The optimal selection problem is dismissed in academic research, which is mainly focused on testing multiple algorithms for solving the optimal loading problem. For instance, the case studies introduced by Chang, Lin & Chuang (2005), Chang (2004) and Chang (2005) on the optimal chiller loading have been extensively analyzed in the literature. Some of the algorithms used to tackle these problems are shown in Table 1.1.

A systematic selection procedure fills the gap in the literature, and its practical benefits are illustrated through applications in chilled water systems as well as in FPSO platforms. The first application is the selection of air-cooled screw chillers in a cooling plant for an air-conditioning system in a commercial building operating 24 hours a day throughout the year. The second application is the selection of a utility plant for a FPSO platform with a forecasted electrical demand over 22 years and a set of reciprocating engines and gas turbines available for selection. In both cases, the performance functions were estimated using the data provided by the manufacturers.

The applications are presented in the form of scientific articles:

- **Article 1:** An optimization scheme for chiller selection in cooling plants.

  Status: Published in the Journal of Building Engineering - ISSN: 2352-7102 - (PARGAS-CARMONA et al., 2022).

- **Article 2:** Optimal selection of utility plants in oil and gas offshore platforms.

  Status: Published in the Journal of the Brazilian Society of Mechanical Sciences and Engineering - ISSN: 1806-3691 - (PARGAS-CARMONA et al., 2023).

Although there is a vast literature on the optimal loading of units that have been previously selected, the selection procedure itself is a topic that has been neglected in these fields. Besides the contribution to the current state of knowledge, the procedure may also be extended to other applications. This way of addressing the issue opens up a research field for exploring the use of different optimization algorithms in the selection problem.

1.4 Structure of the thesis

Chapter 1 presents the context of the problem as well as the justification and objectives of the study. This is followed by the description of the structure of the thesis.

Chapter 2 presents the technical underpinnings of the proposed procedure. The mathematical formulation is outlined and two alternative approaches to solve the problem are discussed.

Chapter 3 presents the problem of selecting chillers in a cooling plant.

Table 1.1: Optimization algorithms used to solve the chiller loading problems introduced by Chang, Lin & Chuang (2005), Chang (2004) and Chang (2005)

Optimization algorithm	Publication	3 x 800 TR (Chang, Lin & Chuang (2005))	2 x 450 TR and 2 x 1000 TR (Chang (2004))	4 x 1280 TR and 2 x 1250 TR (Chang (2005))
Simulated annealing (SA)	Chang (2006)			X
Continuous genetic algorithm / Particle swarm optimization (PSO)	Ardakani, Ardakani & Hosseinian (2008)			X
Evolution strategy (ES)	Chang et al. (2009)			X
Particle swarm optimization (PSO)	Lee & Lin (2009)	X	X	
Gradient method (GM)	Chang, Chan & Lee (2010)	X	X	
Differential evolution (DE)	Lee, Chen & Kao (2011)	X	X	
Improved firefly algorithm (IFA)	Coelho & Mariani (2013)	X		X
Differential search (DS)	Sulaiman et al. (2014)			X
Differential cuckoo search algorithm (DCSA)	Coelho et al. (2014)	X	X	X
Elitism-based PSO (EPSO) / Multi-agent PSO (MA-PSO)	Askarzadeh & Coelho (2015)	X		
Teaching-learning-based optimization (TLBO)	Duan et al. (2018)	X	X	X
Improved invasive weed optimization (IIWO)	Zheng & Li (2018)	X	X	X
Exchange market algorithm	Sohrabi et al. (2018)	X	X	X
Improved artificial fish swarm algorithm (VAFSA)	Zheng, Li & Duan (2019)	X	X	X
Improved particle swarm optimization (IPSO)	Tian et al. (2019a)	X		
Improved grasshopper optimization algorithm (GOA)	Wenhan et al. (2019)	X	X	X
Camel traveling behavior algorithm	Wenhan et al. (2019)	X		
Augmented group search optimization (AGSO)	Teimourzadeh, Jabari & Mohammadi-Ivatloo (2020)	X	X	X
Distributed chaotic estimation of distribution algorithm (DCEDA)	Yu et al. (2020)	X		X
Imperialistic competitive algorithm	Jabari, Mohammadpourfard & Mohammadi-ivatloo (2020)	X	X	X
Quantum emperor penguin optimisation algorithm	Min, Tang & Rouyendegh (2020)	X	X	X

Chapter 4 presents the problem of selecting utility plants in an oil and gas offshore platform.

Chapter 5 presents the final considerations and the overall findings. It is also discussed how the procedure proposed may be applied in other contexts.

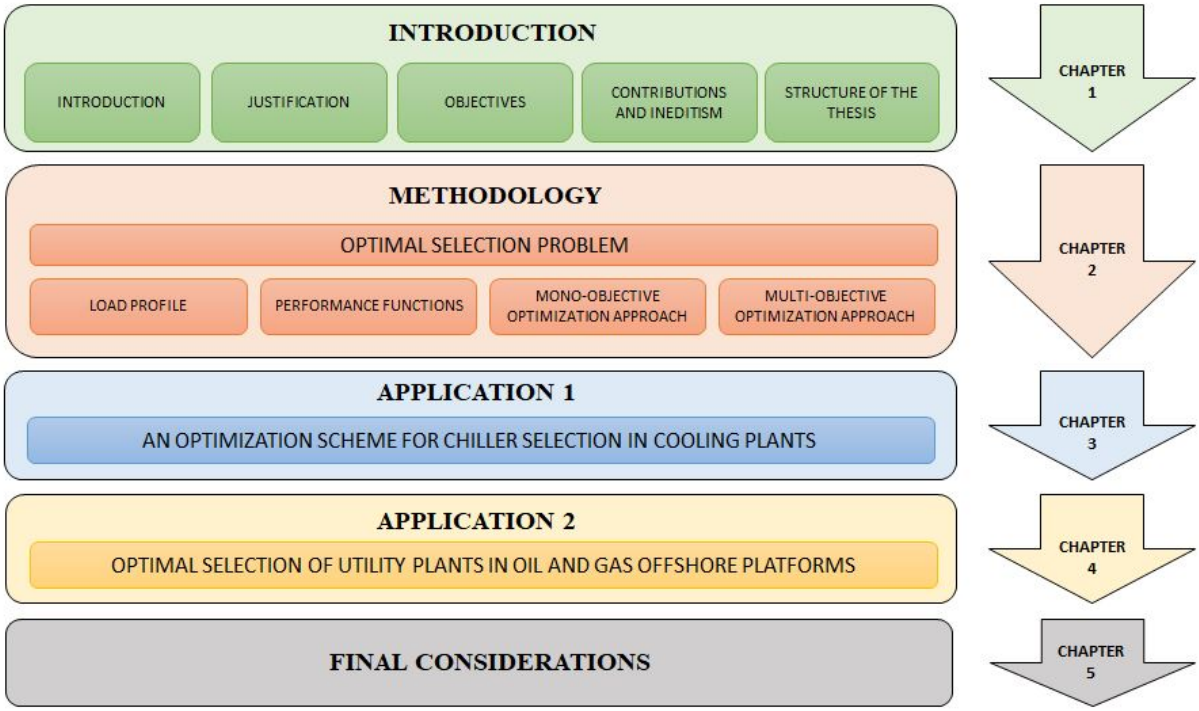

Figure 1.1: Structure of the thesis

Chapter 2

Methodology

In order to formulate the selection problem in mathematical terms, it is necessary to forecast the load demand over the lifespan of the system, as well as to estimate the performance functions of the units available for selection. Using convenient approximations may reduce the computational cost of the problem without significant prejudice. In any case, two approaches to the optimal selection problem are presented: a mono-objective optimization with a single cost-based function, and a multi-objective optimization with two objective functions each based on either capital cost or energy consumption. The second approach is intended to produce a set of nondominated solutions that would allow the engineers to conduct a subsequent trade-off analysis. The selection procedure is summarized in Figure 2.1.

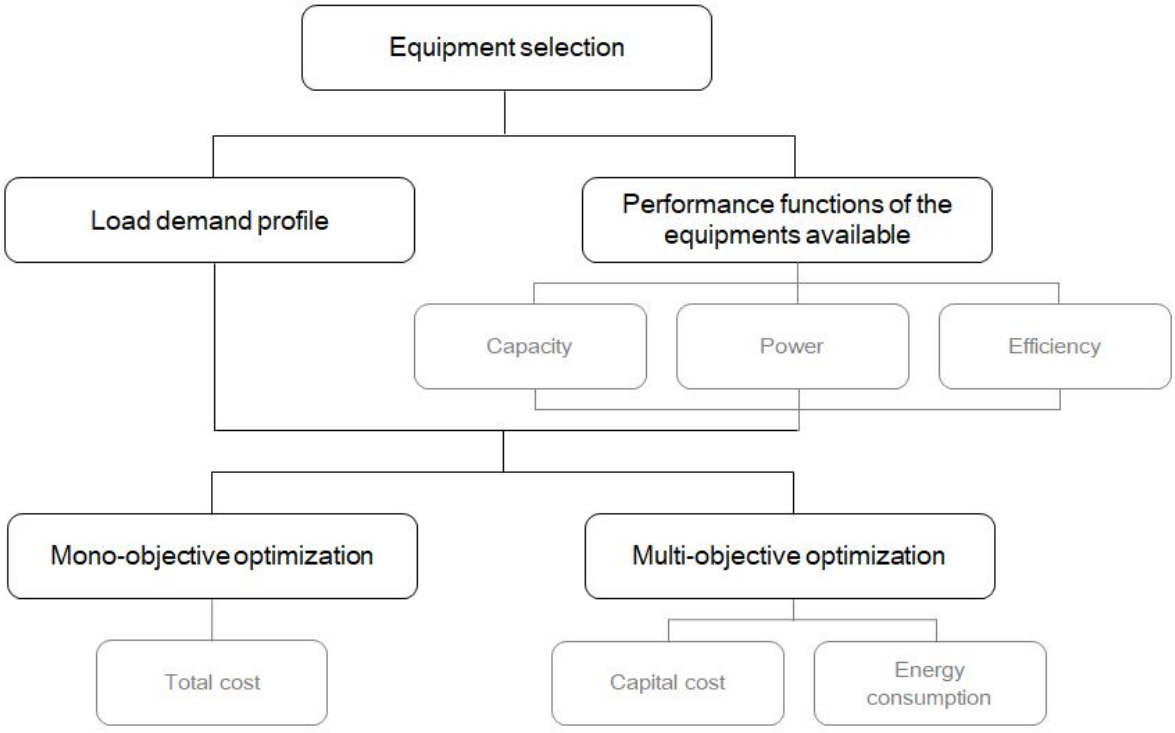

Figure 2.1: Selection procedure

2.1 Load profile

Historical data records provide useful information for estimating the load demand throughout the lifespan of the system. Since the load demand changes over time, analyzing the load profile is a better strategy than using the peak load as the design condition. A method that account for the load fluctuations is sorting the load forecast into equally sized bins, which are discrete groups that represent the time within a certain range of demand. Thus, instead of using a single peak-load condition for an entire period, the analysis can be made for all bin conditions. The selection procedure proposed in this chapter requires the load profile over the period under analysis; however, discussing the methods for estimating the load demand is out of the scope of this thesis.

2.2 Performance functions

The performance data provided by the manufacturer, for example, the chiller performance data of the screw chillers that can be seen in Appendix A, is a crucial for building the models that will be utilized in the optimal selection problem. The performance models may be approached either as the capacity and power consumption functions or as the efficiency functions depending on the data available.

2.2.1 Capacity functions

The actual capacity ϕ_{ij} of a unit i at certain level of demand j is a proportion R_{ij} (partial load ratio) of the full capacity k_i (Equation 2.1).

$$\phi_{ij} = k_i R_{ij} \tag{2.1}$$

In some cases, other variables may affect the capacity of a unit. For instance, the capacity curves of a chiller (Appendix B) show that the capacity model should include slope changes according to the outdoor temperature T_j (Equation 2.2).

$$\phi_{ij} = (\alpha_{1i} + \alpha_{2i} T_j) R_{ij} \tag{2.2}$$

The parameters α_{1i} and α_{2i} may be estimated by using Ordinary Least Squares.

2.2.2 Power functions

The power ψ_{ij} required by a unit i at certain level of demand j may be estimated as a quadratic function of the partial load ratio as can be seen in the performance curves (Appendix B). It may be modeled as shown in Equation 2.3.

$$\psi_{ij} = \beta_{0i} + \beta_{1i} R_{ij} + \beta_{2i} R_{ij}^2 \tag{2.3}$$

The outdoor temperature T_j may be included in the model by a complete second degree polynomial function (Equation 2.4).

$$\psi_{ij} = \beta_{0i} + \beta_{1i} T_j + \beta_{2i} T_j^2 + \beta_{3i} R_{ij} + \beta_{4i} R_{ij}^2 + \beta_{5i} R_{ij} T_j \tag{2.4}$$

A simplified version of a power model that is useful for reducing complexity in the optimization problem is shown in Equation 2.5.

$$\psi_{ij} = \beta_{0i} + \beta_{1i} T_j + \beta_{2i} R_{ij} + \beta_{3i} R_{ij} T_j \tag{2.5}$$

The parameters β_{0i}, β_{1i}, β_{3i}, β_{4i} and β_{5i} may be estimated by using Ordinary Least Squares.

2.2.3 Efficiency functions

An ordinary practice in some contexts for measuring the performance of a unit i at certain level of demand j is estimating the efficiency η_{ij}. It may be modeled as shown in Equation 2.6

$$\eta_{ij} = \beta_{1i} \cdot R_i j^2 + \beta_{2i} \cdot R_{ij} + \beta_{3i} \tag{2.6}$$

The parameters β_{0i}, β_{1i} and β_{3i} may be estimated by using Ordinary Least Squares.

2.2.4 Goodness of fit of the performance models

The goodness of fit of a performance model may be evaluated by the the coefficient of determination or R-squared (Equation 2.7), which is the proportion of the total variance ($\sum_{i=1}^{n}(Y_t - \bar{Y})^2$) that is explained by the variance of the linear regression model ($\sum_{i=1}^{n}(\hat{Y}_i - \bar{Y})^2$).

$$\text{R-squared} = \frac{\sum_{i=1}^{n}(\hat{Y}_i - \bar{Y})^2}{\sum_{i=1}^{n}(Y_t - \bar{Y})^2} \tag{2.7}$$

Comparing the goodness of fit of performance models with different number of independent variables may be misleading because the R-squared increases when a new predictor is added to the model. In order to avoid this problem, it is used the adjusted R-squared (Equation 2.8), that takes into account both the number of predictors (k) in the model and the sample size (n).

$$\text{Adjusted R-squared} = 1 - \frac{(1 - \text{R-squared})(n-1)}{n-k-1} \tag{2.8}$$

2.3 Mono-objective optimization approach

2.3.1 Objective function

Given a system designed to operate with N units at P levels of demand, the goal is to minimize both the operating cost and the capital cost. The former is obtained by multiplying the total consumption at each level of demand by the energy price (w_1); the latter is obtained by multiplying the sum of the acquisition cost (c_i) of the units selected ($S_{ik} = 1$) by the depreciation rate (w_2). The total power required at each level of demand (g_j) is the sum of the power required from each unit i operating at the level of demand j (ψ_{ij}). This has to be multiplied by the corresponding operating time (t_j) in order to obtain the energy consumption. The objective function may be formulated as the minimization of Equation 2.9.

$$f(S, R) = w_1 \sum_{j=1}^{P} g_j t_j + w_2 \sum_{i=1}^{C} \sum_{k=1}^{N} S_{ik} c_i \tag{2.9}$$

The objective function also may be formulated taking into account the time value of money by computing the net present value of the operating cost at each level of demand j with an interest rate r. In this case, the first term of the objective function is expressed as shown in Equation 2.10.

$$\text{Operating cost} = w_1 \sum_{j=1}^{P} \frac{g_j t_j}{(1+r)^j} \tag{2.10}$$

2.3.2 Constraints

The total capacity at each level of demand (h_j) is the sum of the capacity of each unit i operating at the level of demand j (ϕ_{ij}). A fundamental constraint is that this capacity has to be greater or equal than the load demand (d_j) at each level (Equation 2.11).

$$h_j \geq d_j \tag{2.11}$$

Another important constraint is that the partial load ratio (R_{ij}) has to be greater or equal than the minimum value m specified by the manufacturer. The operating range of unit i is defined by Equation 2.12.

$$\text{Operating range} = \{0\} \bigcup [m_i; 1] \tag{2.12}$$

Besides the constraints of capacity and operating range, other constraints either related to the specific application or required by the syntax of the computer code might emerge.

2.3.3 Optimization method

The optimal selection problem formulated as described in this section constitutes a mixed integer nonlinear problem (MINLP) that can be coded in AMPL format (FOURER, 1996) and submitted to NEOS Server (Czyzyk; Mesnier; Moré, 1998; Dolan, 2001; Gropp; Moré, 1997) to be solved using BARON (TAWARMALANI; SAHINIDIS, 2005; SAHINIDIS, 2017). This is the solver used in the MINLP applications presented in Chapters 3 and 4, but the choice of the software will depend on the specific needs.

2.4 Multi-objective optimization approach

2.4.1 Objective functions

The optimal selection problem may be formulated with two objectives to be minimized: capital cost and energy consumption. Dealing with the energy consumption in its original units instead of monetary units may be a better decision under highly-variable prices. It may be also convenient when the capital cost and the operating cost are assumed by different agents.

Objective function 1: Energy consumption

Given the operating time at each level of demand (t_j), the objective function for energy consumption is formulated as the sum of the individual consumptions (Equation 2.13). The actual power consumption (g_{ij}) of unit i at level j is the product of the estimated consumption (ψ_{ij}) and the power status binary variable (P_{ij}). By doing so, the result will be zero when the unit is turned off. Otherwise, the result will be given by the consumption function.

$$f_1(S, R) = \sum_{j=1}^{p} \sum_{i=1}^{q} g_{ij} t_j \tag{2.13}$$

The actual power consumption (g_{ij}) is obtained from Equation 2.14.

$$g_{ij} = P_{ij} \psi_{ij} \tag{2.14}$$

Objective function 2: Capital cost

The total capital cost is obtained from the sum of each cost (c_i) of the N units selected for the system (Equation 2.15).

$$f_2(S, R) = \sum_{i=1}^{N} c_i \tag{2.15}$$

It is worth pointing out the difference between the power status variable and the selection variable. The former is a binary variable that is equal to 0 when the unit is turned off and it is equal to 1 when the unit is turned on. It is useful when a discontinuous operating range, such as Eq. 2.12, is not allowed by the optimization software. The latter indicates the model that has been selected. It may be either a binary variable (selected/not selected) or an nominal variable that indicates the model selected.

2.4.2 Constraints

The feasible region is determined by Equation 2.16. This set of constraints ensures that the demand d_j at each level j will be satisfied by the total capacity, which is the sum of the actual capacity of each unit operating at that level.

$$\sum_{i=1}^{N} h_{ij} \geq d_j \tag{2.16}$$

As well as in the case of power consumption functions, Equation 2.17 establishes that the actual capacity h_{ij} of unit i at level of demand j is given by the estimated capacity ϕ_{ij} multiplied by de power status binary variable P_{ij}.

$$h_{ij} = P_{ij}\phi_{ij} \tag{2.17}$$

2.4.3 Optimization method

A broad variety of algorithms can be used to solve the optimal selection problem proposed in this section. Although other alternatives can be explored, the algorithm used in the applications presented in Chapters 3 and 4 is NSGA-II (Nondominated Sorting Genetic Algorithm II) with single point crossover and integer flip mutation operators. This is a well-known algorithm that suits the optimal selection problem and its advantages are acknowledged in the literature ((KHARE; YAO; DEB, 2003), (HIDALGO et al., 2008), (MONSEF et al., 2019)).

There are two important goals expected from a multiobjective optimization algorithm: convergence to the optimal set of solutions and good diversity of solutions. In this regard, Deb et al. (2002) concluded that NSGA-II was able to maintain a better spread of solutions and converge better in the obtained nondominated front when compared to other multiobjective optimization algorithms. Additionally, Sayyad & Ammar (2013) found that NSGA-II was the algorithm of choice in 53% of the papers analyzed in a literature survey of studies that used multiobjective optimization.

Algorithm parameters

The chromosome is expressed as a string of $N + 2Np$ decision variables as follows: N selection variables (S_i), Np power status variables (P_{ij}) and Np partial load ratio variables (R_{ij}).

Even though it is not made any formal attempt to find the best parameter setting in the seminal paper of Deb et al. (2002), the parameters recommended are a crossover probability of $p_c = 0.9$ and a mutation probability of $p_m = 1/(N+2Np)$ (1 divided by the number of decision variables). The population size and the number of generations may be established after experimentation.

In general, it has been given little attention to constrained multiobjective optimization in evolutionary algorithms. One useful constraint-handling strategy consists of including a penalty factor in order to worsen the fitness values when the constraints are not satisfied. This penalty factor has to be large enough to prevent infeasible solutions from being in the set of solutions, but not too large so the algorithm is forced to converge without sufficiently exploring the search space. This issue is particularly critical under strong parameter interactions. Experiments have to be performed to analyze the effects of different settings.

2.4.4 Pareto dominance

A general optimization problem may be defined by the following elements: a search space X; an objective space Z; and a function $f : X \to Z$ that assigns an objective vector $\mathbf{z} \in Z$ to each decision vector $\mathbf{x} \in X$. The goal is to find a solution $\mathbf{x}^* \in X$ mapped to a minimum $\mathbf{z}^* \in Z$. In the case of a mono-objective optimization, the "less or equal than" operator ($\leq$) is a total order in the objective space because $Z = \mathbb{R}$ and any to elements $\mathbf{z}^i$ and $\mathbf{z}^j$ are comparable. On the other hand, in the case of a multi-objective optimization problem it is used the operator $\preceq$ as an extension of $\leq$ in $\mathbb{R}^n$ since multiple minimum solutions may be found with different trade-off between the individual functions in $f = (f_1, f_2, ..., f_n)$.

Some preference relations on the objective vectors are:

- The relation $\mathbf{z}^1 \preceq \mathbf{z}^2$ represents a weak Pareto dominance, i.e. $\mathbf{z}^1$ weakly dominates $\mathbf{z}^2$ because $\mathbf{z}^1$ is not worse than $\mathbf{z}^2$ in all objectives.

- The relation $\mathbf{z}^1 \prec \mathbf{z}^2$ represents a Pareto dominance, i.e. $\mathbf{z}^1$ dominates $\mathbf{z}^2$ because $\mathbf{z}^1$ is not worse than $\mathbf{z}^2$ in all objectives and better in at least one objective.

- The relation $\mathbf{z}^1 \prec\prec \mathbf{z}^2$ means that $\mathbf{z}^1$ strictly dominates $\mathbf{z}^2$ because $\mathbf{z}^1$ is better than $\mathbf{z}^2$ in all objectives.

- The relation $\mathbf{z}^1 \parallel \mathbf{z}^2$ means that $\mathbf{z}^1$ and $\mathbf{z}^2$ are incomparable because neither $\mathbf{z}^1 \preceq \mathbf{z}^2$ nor $\mathbf{z}^2 \preceq \mathbf{z}^1$.

- The relation $\mathbf{z}^1 \sim \mathbf{z}^2$ means that $\mathbf{z}^1$ and $\mathbf{z}^2$ are indifferent because $\mathbf{z}^1$ and $\mathbf{z}^2$ have the same values in the objectives.

Quality metrics

Comparing solutions under a mono-objective approach is straightforward, but a multi-objective requires a quality metric. A useful alternative to measure de quality of a set of nondominated solutions of a multi-objective optimization is the hypervolume indicator, which is the volume covered by the elements of a nondominated set W (DEB, 2009). Let v_i be the volume enclosed by $w_i \in W$ relative to a reference point, then the hypervolume I_H is calculated as follows:

$$I_H(W) = \bigcup_{1}^{|W|} v_i \tag{2.18}$$

In order to assess the quality of a set of nondominated solutions, a reference set R may be used as follows:

$$I_H^-(W) = I_H(R) - I_H(W) \tag{2.19}$$

Smaller values of $I_H^-(W)$ indicates better quality. When the reference set is not given, then $I_H(R)$ may be considered to be zero.

Chapter 3

Application 1

3.1 Article 1: An optimization scheme for chiller selection in cooling plants

Authors

Luis A. Pargas-Carmona[a], Júlio A. M. Da Silva[b], Ângelo M. O. Sant'Anna[b], José L. Risco-Martín[c].

(a) Department of Production Engineering, Federal University of Western Bahia, R/Itabuna 1278, Santa Cruz, Luís Eduardo Magalhães (Bahia) 47850-000, Brazil.

(b) Department of Mechanical Engineering, Federal University of Bahia - Polytechnic School, R/Prof. Aristides Novis 2, Federação, Salvador (Bahia) 40210-630, Brazil.

(c) Department of Computer Architecture and Automation, Complutense University of Madrid, C/Prof. José García Santesmases 9, Madrid 28040, Spain.

Abstract

Providing effective cooling for buildings and industrial facilities at minimum cost is one of the main challenges in the HVAC industry. Considerable effort has been put into the optimization of existing cooling plants, but the chiller selection procedure has been relegated to a second place. This paper introduces two alternative formulations to add the chiller selection into the overall optimization problem: i) a mathematical programming approach with a single cost-based objective function and ii) a multi-objective optimization of capital cost and energy consumption. It was analyzed the case of a cooling plant with a known load profile and 13 air-cooled screw chiller models ranging from 140 to 500 TR available for purchase. The minimum objective value in the mathematical programming

approach is obtained by selecting three 500 TR chillers. On the other hand, the multi-objective optimization approach produced a set of nine nondominated solutions (including the three 500 TR chiller selection). Under the second approach it is not necessary to translate the energy consumption into monetary terms. The results of both alternatives are considerable different from the straightforward approach of selecting chillers with total nominal capacity closer to the peak load (900 TR). This reveals the importance of a formal selection procedure.

Keywords: Mathematical programming; Multi-chiller systems; Multi-objective optimization; Optimal chiller selection.

3.1.1 Introduction

Air-conditioning systems generally demand more energy than any other system in commercial and office buildings. According to Thangavelu, Myat & Khambadkone (2017) the cooling load accounts for 45-60% of the total energy consumption. In many tropical countries this percentage may be even higher. The cooling demand in buildings may vary according to several factors, such as: outdoor temperature, occupancy level, activity type, etc. Multi-chiller systems provide flexibility to operate under conditions of high variability because they enable the switching on and off of the chillers when required. They also have lower energy consumption under partial load conditions compared to single-chiller systems. The examination of the thermal load variations throughout the year allows engineers to make design decisions based on the whole load profile instead of exclusively on the peak load, which is usually an exceptional condition.

Providing effective cooling for buildings and industrial facilities at minimum cost is one of the main challenges in the HVAC industry. It is known that the chiller performance varies substantially according to the outdoor temperature and the Partial Load Ratio (PLR), i.e. the actual cooling capacity of the chiller divided by its maximum capacity at the same conditions. Consequently, the chiller selection and the operating conditions are essential aspects that have to be considered in the design of cooling plants.

Much of the literature focused on finding the Optimal Chiller Loading (OCL), i.e. the load share of each chiller that minimizes the overall energy consumption for previously selected chillers. As a matter of fact, many authors refer to this problem as "economic dispatch of chiller plants" (CHANG; CHAN; LEE, 2010; LO; TSAI; LIN, 2016; SOHRABI et al., 2018; TEIMOURZADEH; JABARI; MOHAMMADI-IVATLOO, 2020; JABARI; MOHAMMADPOURFARD; MOHAMMADI-IVATLOO, 2020). It is necessary to take a step back and acknowledge that once the cooling needs are understood and a preliminary design of the plant is outlined, the next move is the chiller selection. There are a few rules of thumb for selecting chillers, such as distributing the peak load evenly into the units of the system, or breaking the load profile down into time-based discrete groups to which

the units are arbitrarily assigned according to their nominal capacities. Both approaches disregard the performance functions and the operating conditions.

The literature is concentrated mainly on testing different optimization algorithms on the same OCL problems: the case presented by Chang (2004), consisting of two 450 TR chillers and two 1000 TR chillers; the case presented by Chang, Lin & Chuang (2005), consisting of three 800 TR chillers; and the case presented by Chang (2005), consisting of four 1280 TR chillers and two 1250 TR chillers. Some authors addressed this problem with bio-inspired algorithms. Recent examples in this category are Improved Invasive Weed Optimization (ZHENG; LI, 2018), Improved Artificial Fish Swarm Algorithm (ZHENG; LI; DUAN, 2019), Improved Grasshopper Optimization Algorithm (WENHAN et al., 2019), Quantum Emperor Penguin Optimization Algorithm (MIN; TANG; ROUYENDEGH, 2020), Improved Particle Swarm Optimization (TIAN et al., 2019b) and Camel Traveling Behavior Algorithm (CHEN et al., 2020). Besides the algorithms based on biological mechanisms, other alternatives have been explored, such as Imperialistic Competitive Algorithm (JABARI; MOHAMMADPOURFARD; MOHAMMADI-IVATLOO, 2020), Teaching-Learning-Based Optimization (DUAN et al., 2018), Exchange Market Algorithm (SOHRABI et al., 2018) and Distributed Chaotic Estimation of Distribution Algorithm (YU et al., 2020).

The design and the scheduling may be simultaneously addressed. This way of tackling these problems is found in other fields. For instance, in Fumero, Corsano & Montagna (2013) an optimization model is proposed for the simultaneous design and scheduling of flowshop plants, and in Pruitt et al. (2014) it is presented a model for determining the configuration, capacity and operational schedule of a distributed generation system at the globally minimum total cost. However, the chiller selection has been overlooked in the literature on the OCL problem. This paper presents two different optimization approaches to deal with the chiller selection problem and the OCL problem at the same time: i) a mathematical programming approach with a single cost-based objective function and ii) a multi-objective optimization of capital cost and energy consumption.

The procedure outlined in this paper seeks to find the best equipment selection by weighing up the trade-off between capital costs and operational costs. This is a problem that has to be managed in many engineering contexts. Nevertheless, selecting the units and designing the operation plan are commonly addressed as if they were separated problems. The main novelty of this work is integrating the chiller selection into the optimal chiller loading problem. This optimization scheme is a formal alternative to less effective rules of thumb commonly used in the HVAC industry, and it may also be applied to other engineering systems as long as the performance functions and the demand profile are known.

3.1.2 Methodology

Given a list of C chiller models available for purchase and their corresponding performance functions (capacity and consumption), a selection of a set of N chillers has to be made in order to guarantee that the cooling load demand will be satisfied at minimum cost. The PLR is included in the analysis as a decision variable. As a result, the optimal chiller selection and the OCL are obtained simultaneously.

Chiller performance functions

The performance functions presented in this section may be useful for both air-cooled chillers and water-cooled chillers with cooling towers. In the first case, the outdoor temperature to be considered is the dry-bulb temperature. In the latter case, the outdoor temperature to be considered is the wet-bulb temperature.

Capacity functions. The capacity (ϕ_{ij}) of a chiller i at certain level of demand j is determined by the outdoor temperature (T_j) and the PLR (R_{ij}). Estimating the capacity of a chiller as its nominal capacity multiplied by the PLR is a poor solution. The capacity may be modeled as a linear function of the PLR with slope changes according to the outdoor temperature. In fact, this model has a perfect fit (as can be seen in Table 3.3). The parameters α_{1i} and α_{2i} in Equation 4.3 may be estimated by using Ordinary Least Squares (OLS).

$$\phi_{ij} = (\alpha_{1i} + \alpha_{2i} T_j) R_{ij} \tag{3.1}$$

Consumption functions. The power consumption (ψ_i) of a chiller i at certain level of demand j is also determined by the outdoor temperature (T_j) and the PLR (R_{ij}). The consumption curves of a typical screw chiller may be modeled as complete second degree polynomial functions. The parameters β_{0i}, β_{1i}, β_{2i}, β_{3i}, β_{4i} and β_{5i} in Equation 3.2 may be estimated by using OLS.

$$\psi_{ij} = \beta_{0i} + \beta_{1i} T_j + \beta_{2i} T_j^2 + \beta_{3i} R_{ij} + \beta_{4i} R_{ij}^2 + \beta_{5i} R_{ij} T_j \tag{3.2}$$

The linear function shown in Equation 3.3, which is a linear model with one interaction term, is also considered for the sake of comparison. The parameters β_{0i}, β_{1i}, β_{2i} and β_{3i} in Equation 3.3 may be estimated by using OLS.

$$\psi_{ij} = \beta_{0i} + \beta_{1i} T_j + \beta_{2i} R_{ij} + \beta_{3i} R_{ij} T_j \tag{3.3}$$

Modeling the performance functions requires empirical data to analyze the variables involved and their functional relationship. Some authors estimate the chiller consumption

as a quadratic function of the PLR (CHANG, 2005), and others use a third degree polynomial model (CHANG, 2004; CHANG; LIN; CHUANG, 2005). However, the outdoor temperature is an important variable that is usually left out of these models. In this paper, the outdoor temperature is included in the analysis because, as will be discussed later, it is a refinement that increases significantly the explanatory power of the model.

Mathematical programming approach

Objective function. The sum of the total consumptions at each level of demand (g_j) may be expressed in monetary terms by multiplying it by the electricity price (w_1). Likewise, the total capital cost, which is the sum of the capital cost (c_i) of each chiller selected ($S_{ik} = 1$), is multiplied by the annual depreciation rate (w_2), that is the proportion at which the chiller is depreciated based on its estimated useful life. In this way both functions are formulated in a year time span as in Equation 3.4.

$$\text{Objective value} = w_1 \sum_{j=1}^{P} g_j + w_2 \sum_{i=1}^{C} \sum_{k=1}^{N} S_{ik} c_i \tag{3.4}$$

Constraints. The binary variable S_{ik} assumes the value of 1 when the model i was selected for chiller k, and assumes the value of 0 otherwise. Equation 3.5 establishes that there is one chiller model for each chiller selected. This does not prevent the chillers selected from having the same model.

$$\sum_{i=1}^{C} S_{ik} = 1 \tag{3.5}$$

Equation 3.6 guarantees that the PLR (R_{ijk}) will be zero when the chiller is not selected.

$$R_{ijk} \leq S_{ik} \tag{3.6}$$

The actual power consumption is equal to the estimated power consumption when the chiller is turned on, and is equal to 0 when the chiller is turned off. Eq. 3.5 and Eq. 3.6 are fundamental constraints for the selection problem. The auxiliary variables θ_{ijk} (continuous) and γ_{ijk} (binary) in Equations 3.7 and 3.8 guarantee that the consumption is zero when the chiller is turned off. The PLR lower limit is represented by r.

$$R_{ijk} \leq \gamma_{ijk} \leq R_{ijk} + 1 - r \tag{3.7}$$

$$\theta_{ijk} = (\beta_{1i} + \beta_{2i} T_j + \beta_{3i} {T_j}^2) \gamma_{ijk} \tag{3.8}$$

The total consumption at level of demand j is obtained from Equation 3.9.

$$g_j = \sum_{i=1}^{C} \sum_{k=1}^{N} (\theta_{ijk} + \beta_{4i} R_{ijk} + \beta_{5i} {R_{ijk}}^2 + \beta_{6i} R_{ijk} T_j) t_j \tag{3.9}$$

The total capacity at level of demand j (h_j) is obtained from Equation 3.10.

$$h_j = \sum_{i=1}^{C} \sum_{k=1}^{N} (\alpha_{1i} + \alpha_{2i} T_j) R_{ijk} \tag{3.10}$$

Equation 3.11 guarantees that the cooling demand (d_j) will be satisfied by the cooling capacity at all levels of demand.

$$h_j \geq d_j \tag{3.11}$$

Multi-objective optimization approach

Multi-objective optimization is a useful alternative for problems that involve more than one objective. When these objectives are conflicting it is desirable to obtain a solution that provides the best compromise between them. Under this approach, the objectives may have different units and it is not necessary to translate the energy consumption into monetary terms.

First objective: energy consumption. Given the time at each level of demand (t_j), the objective function for energy consumption (Equation 3.12) is formulated as the time-weighted sum of the chiller consumptions. The actual consumption (g_{ij}) of chiller i at level of demand j is obtained by multiplying the estimated consumption function by the chiller power status binary variable (P_{ij}). This ensures that the results will be zero when the chiller is turned off.

$$\text{Objective value } 1 = \sum_{j=1}^{p} \sum_{i=1}^{q} g_{ij} t_j \tag{3.12}$$

Second objective: capital cost. The capital cost (Equation 3.13) is calculated as the sum of the costs of the N chillers selected ($S_i = 1$).

$$\text{Objective value } 2 = \sum_{i=1}^{N} c_i \tag{3.13}$$

Constraints. The feasible region is determined by a set of constraints (Equation 3.14) that ensure that the cooling demand (d_j) will always be satisfied by the cooling capacity (h_{ij}). Just as is the case for the consumption, the actual cooling capacity of chiller i at

Table 3.1: Cooling load profile

Level	Duration	Cooling demand	Outdoor temperature
1	2190 h	200 TR	82°F (27.8°C)
2	730 h	300 TR	82°F (27.8°C)
3	365 h	600 TR	82°F (27.8°C)
4	1095 h	700 TR	82°F (27.8°C)
5	1460 h	700 TR	86°F (30.0°C)
6	365 h	800 TR	86°F (30.0°C)
7	1460 h	800 TR	90°F (32.2°C)
8	1095 h	900 TR	90°F (32.2°C)

Table 3.2: Cost of the chiller models available for purchase

Nominal capacity (TR)	Cost (USD)
140	117676.40
160	124725.20
180	129795.20
200	137354.40
225	144197.20
250	154227.60
275	161888.40
300	173463.60
325	186584.40
350	217310.80
400	239306.40
450	258177.20
500	281070.80

level of demand j is given by the capacity function (ϕ_{ij}) multiplied by the chiller power status variable (P_{ij}).

$$\sum_{i=1}^{N} h_{ij} \geq d_j \tag{3.14}$$

3.1.3 Case study

The selection scheme is tested on a cooling plant with the load profile summarized in Table 3.1. It corresponds to an air-conditioning system for a commercial building operating 24 hours a day throughout the year.

The number of chillers must be between 2 and 6 in order not to exceed the space allowed. There are 13 air-cooled screw chiller models ranging from 140 to 500 TR available for purchase. According to the manufacturer, these chillers can take on any PLR value from 15% to 100%. The chiller models and their costs are indicated in Table 3.2.

The performance data and the cost of the chillers were provided by the manufacturer for research purposes under the condition of anonymity. The performance curves for

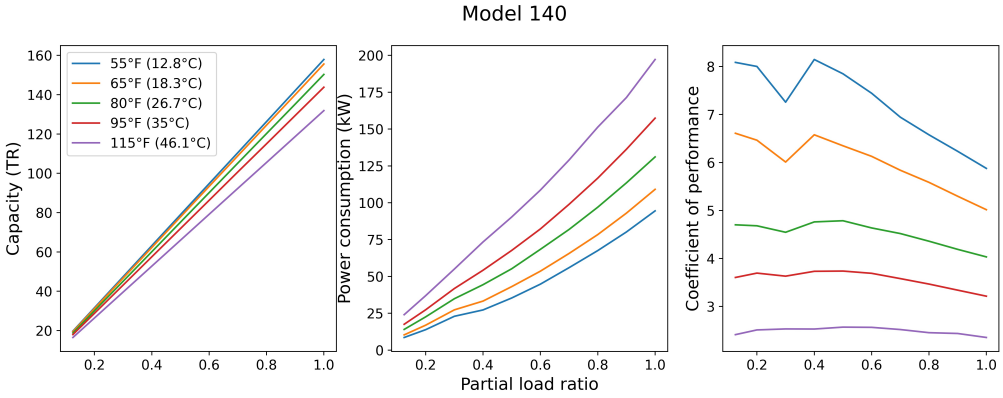

Figure 3.1: Performance curves for Model 140

Table 3.3: Goodness of fit (Adjusted R-squared) of the performance models

Nominal capacity (TR)	**Capacity**	**Consumption**	
		Quadratic	**Linear**
140	1.000	0.999	0.991
160	1.000	0.999	0.990
180	1.000	0.999	0.987
200	1.000	0.999	0.983
225	1.000	0.999	0.988
250	1.000	0.999	0.991
275	1.000	0.999	0.990
300	1.000	0.999	0.988
325	1.000	0.999	0.985
350	1.000	0.999	0.987
400	1.000	0.998	0.989
450	1.000	0.999	0.987
500	1.000	0.999	0.984

Model 140 are shown in Figure 3.1.

The importance of having a set of curves specifying the chiller performance under various operating conditions is discussed in Yu & Chan (2006). Developing regression-based models for the actual operating conditions is a common practice in this field, e.g. Aravelli & Rao (2013). The outdoor temperature (T_j) is disregarded in the performance models found in most of the literature, e.g. in Chang (2004), Chang, Lin & Chuang (2005), Chang (2005) and the subsequent papers. In this case study, the performance functions were estimated using the manufacturer's data over the operating range including the outdoor temperature. The goodness of fit of Equations 4.3, 3.2 and 3.3 for each of the 13 chiller models available for purchase is shown in Table 3.3. The regression parameters can be seen in Table 3.4.

The electricity cost (w_1) in the single cost-based objective function (Equation 3.4) was set as 0.10 USD/kWh, which is close to the median of the standard variable rate tariff for the Brazilian electricity suppliers (ANEEL, 2021). The annual depreciation rate (w_2) is assumed to be 10%, considering a life expectancy of 10 years and a null salvage value.

Table 3.4: Regression parameters of the performance functions

Nominal capacity (TR)	Capacity		Quadratic			Consumption				Linear			
	α_1	α_2	β_0	β_1	β_2	β_3	β_4	β_5	β_0	β_1	β_2	β_3
140	183.3708	-0.4327	29.3400	-0.6710	0.0043	-53.3100	50.2600	1.6428	-11.3884	0.0620	2.7461	1.6428
160	206.0962	-0.4697	35.3300	-0.8147	0.0052	-61.4400	62.5000	1.7842	-14.3559	0.0727	8.2671	1.7842
180	230.0791	-0.5386	39.4400	-0.8570	0.0054	-78.1500	85.9200	1.9631	-16.7344	0.0579	17.6856	1.9631
200	252.5621	-0.5855	46.3000	-0.9600	0.0059	-96.3600	107.9700	2.1327	-18.3537	0.0403	24.0710	2.1327
225	289.3007	-0.7570	59.5700	-1.4370	0.0093	-80.0000	92.6200	2.3982	-24.9283	0.1506	23.3421	2.3982
250	347.1263	-0.9456	80.0300	-2.1070	0.0138	-62.3800	76.8100	2.8455	-31.1349	0.2436	23.2950	2.8455
275	367.2491	-0.9908	83.7300	-2.1780	0.0142	-71.3900	90.6900	3.0268	-33.3863	0.2425	29.7637	3.0268
300	380.6569	-0.9938	85.3500	-2.1150	0.0135	-92.4400	114.1800	3.0958	-32.4032	0.1843	34.9156	3.0958
325	406.2294	-1.0008	79.0700	-1.8420	0.0117	-128.8800	161.3500	3.3273	-37.1588	0.1458	51.0835	3.3273
350	465.8241	-1.2423	84.1000	-1.9770	0.0130	-122.6000	160.7100	3.6225	-40.8323	0.2332	56.6545	3.6225
400	539.9661	-1.4561	64.7000	-1.5780	0.0111	-107.7000	163.1000	4.0490	-47.7980	0.3062	74.2107	4.0488
450	607.8682	-1.6362	70.9000	-1.7380	0.0125	-128.4000	218.3600	4.2410	-64.1083	0.3920	115.1828	4.2409
500	668.6709	-1.7872	83.3000	-1.8750	0.0125	-169.6000	280.4100	4.7290	-65.4591	0.2404	143.2083	4.7290

Table 3.5: Chiller selection for the MINLP

Number of chillers	Chiller selection	Objective value (USD)
2	2 x 500 TR	510011.46
3	3 x 500 TR	485221.37
4	3 x 500 TR and 1 x 200 TR	487735.69
5	1 x 500 TR, 2 x 325 TR and 2 x 200 TR	491134.61
6	1 x 500 TR, 1 x 325 TR and 4 x 200 TR	495576.49

The reference service life for air-cooled chillers is 15 years according to (STANFORD, 2010), but a reduction factor was applied because of the exposition to rapid oxidation in coastal areas.

3.1.4 Results

Mathematical programming approach

Mixed integer nonlinear optimization problem (MINLP). The problem was submitted to NEOS Server (Czyzyk; Mesnier; Moré, 1998; Dolan, 2001; Gropp; Moré, 1997) in AMPL format (FOURER, 1996) and it was solved using BARON, which is a solver for mixed integer nonlinearly constrained optimization problems (TAWARMALANI; SAHINIDIS, 2005; SAHINIDIS, 2017). The total number of chillers composing the cooling plant was restricted to: 2, 3, 4, 5 and 6. The chiller selection is shown in Table 3.5, and the OCL results can be seen in Table 3.6.

The operating cost surpasses the capital cost for the plant with 2 chillers, and its optimum turned out to be more expensive than the optimum for the plants with 3, 4, 5 and even 6 chillers. The optimum for 3 chillers is the best alternative. This selection consists of three 500 TR units.

Linear approximation. The size of the MINLP increases exponentially with the number of chillers, but if the original consumption functions (Equation 3.2) are replaced by the linear consumption functions (Equation 3.3), the optimization problem may be solved as a linear problem. It is important to bear in mind that the objective value in the new problem has to be corrected afterwards by the original functions. The chiller selection for the linear approximation is shown in Table 3.7, and the corresponding OCL can be seen in Table 3.8.

Even though the linear approximation was not able to find the best solution, the error of this approximation is relatively small (Figure 3.2).

Since the NEOS Server has a time limit of 8 hours, which is less than the time required to solve the MINLP for $N \geq 3$, the best fitting exponential function was used to estimate the execution time. The speedup, i.e. the performance of the linear approximation in

Table 3.6: Optimization results for the MINLP

Number of chillers	Nominal capacity (TR)	Partial Load Ratio								Objective value (USD)
		Level 1	Level 2	Level 3	Level 4	Level 5	Level 6	Level 7	Level 8	
2	500	19%	29%	57%	67%	68%	78%	79%	89%	510011.46
	500	19%	29%	57%	67%	68%	78%	79%	89%	
3	500	19%	19%	38%	45%	45%	52%	53%	59%	485221.37
	500	19%	19%	38%	45%	45%	52%	53%	59%	
	500	0%	19%	38%	45%	45%	52%	53%	59%	
4	500	19%	17%	31%	38%	37%	49%	45%	54%	487735.69
	500	0%	16%	36%	39%	43%	43%	44%	51%	
	500	19%	17%	31%	39%	37%	44%	50%	51%	
	200	0%	20%	43%	47%	48%	50%	49%	56%	
5	200	22%	22%	46%	46%	48%	53%	53%	60%	491134.61
	200	0%	24%	38%	46%	47%	53%	53%	59%	
	325	18%	17%	43%	44%	44%	50%	53%	59%	
	500	19%	18%	34%	44%	44%	51%	50%	57%	
	325	0%	19%	34%	43%	44%	50%	53%	59%	
6	200	15%	18%	37%	40%	47%	52%	45%	57%	495576.49
	325	0%	15%	33%	42%	46%	46%	49%	53%	
	200	15%	19%	44%	38%	41%	53%	45%	57%	
	200	15%	23%	43%	44%	41%	52%	53%	57%	
	200	15%	20%	34%	38%	48%	52%	51%	57%	
	500	15%	17%	33%	45%	38%	45%	50%	55%	

Table 3.7: Chiller selection for the linear approximation

Number of chillers	Chiller selection	Objective value (USD) Original	Corrected
2	1 x 500 TR and 1 x 450 TR	523393.61	526817.55
3	2 x 500 TR and 1 x 450 TR	518972.92	544776.48
4	2 x 500 TR, 1 x 450 TR and 1 x 160 TR	516905.97	548556.71
5	2 x 500 TR and 3 x 160 TR	516982.41	541245.24
6	2 x 500 TR, 1 x 325 TR and 3 x 160 TR	517766.97	559159.93

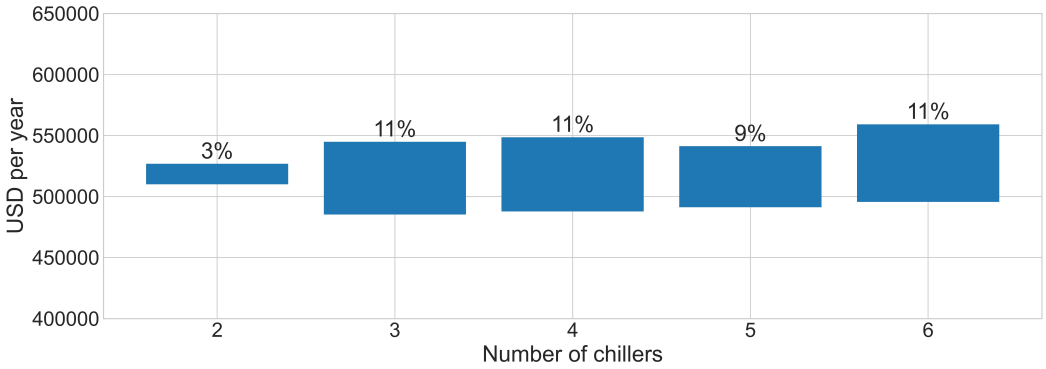

Figure 3.2: Linear approximation error (%)

terms of execution time relative to the original MINLP, is shown in Figure 3.3.

In the MINLP, as well as in the linear approximation, 5 out of the 13 models available can be observed in the results: 160 TR, 200 TR, 325 TR, 450 TR and 500 TR. However, only 2 models are found in the results of both formulations: 325 TR and 500 TR. The optimal selection for 3 chillers using the linear approximation is similar to the selection obtained using the MINLP formulation. In this case, it consists of two 500 TR units and one 450 TR unit instead of three 500 TR units.

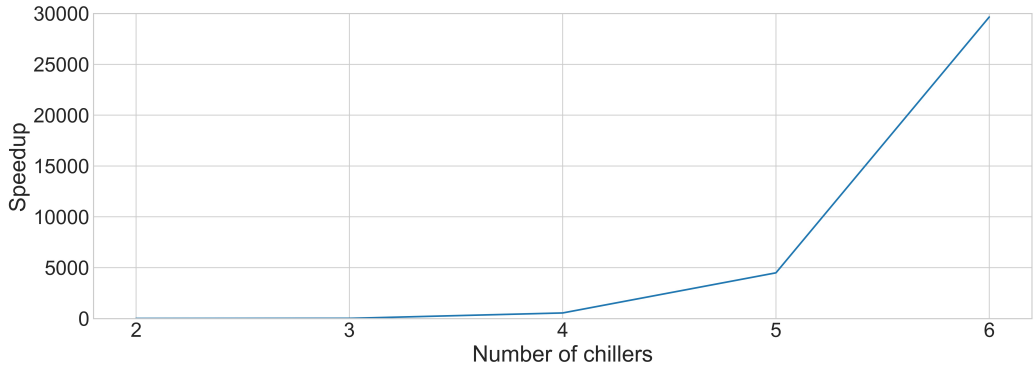

Figure 3.3: Relative performance of the linear approximation in terms of execution time

Table 3.8: Optimization results for the linear approximation

Number of chillers	Nominal capacity (TR)	Partial Load Ratio								Objective value (USD)	
		Level 1	Level 2	Level 3	Level 4	Level 5	Level 6	Level 7	Level 8	Raw	Corrected
2	450	26%	47%	100%	100%	100%	100%	100%	100%	523393.61	526817.55
	500	15%	15%	24%	43%	45%	65%	67%	87%		
3	500	15%	15%	15%	15%	30%	50%	52%	15%	518972.92	544776.48
	450	15%	30%	94%	100%	100%	100%	100%	100%		
	500	15%	15%	15%	28%	15%	15%	15%	72%		
4	500	15%	15%	15%	15%	15%	17%	20%	39%	516905.97	548556.71
	450	0%	15%	58%	79%	81%	100%	100%	100%		
	500	15%	15%	15%	15%	15%	15%	15%	15%		
	160	26%	43%	100%	100%	100%	100%	100%	100%		
5	160	15%	56%	100%	100%	100%	100%	100%	100%	516982.41	541245.24
	500	15%	15%	15%	23%	24%	44%	46%	65%		
	500	15%	15%	15%	15%	15%	15%	15%	15%		
	160	0%	15%	100%	100%	100%	100%	100%	100%		
	160	15%	15%	65%	100%	100%	100%	100%	100%		
6	325	15%	15%	15%	15%	15%	46%	49%	81%	517766.97	559159.93
	500	15%	15%	15%	15%	15%	15%	15%	15%		
	160	0%	27%	100%	100%	100%	100%	100%	100%		
	160	0%	15%	100%	100%	100%	100%	100%	100%		
	500	15%	15%	15%	15%	15%	15%	15%	15%		
	160	0%	15%	36%	95%	100%	100%	100%	100%		

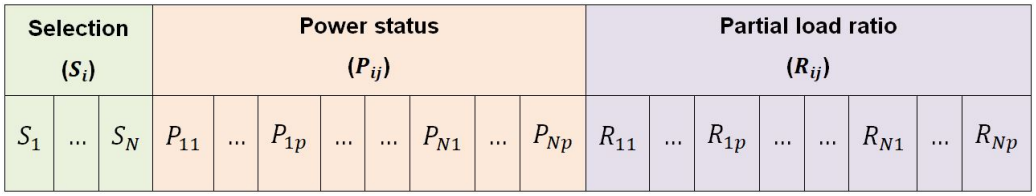

Figure 3.4: Chromosome specification

Table 3.9: NSGA-II algorithm parameters

Number of generations	G
Population size	100
Chromosome length	51
Probability of crossover	0.9
Probability of mutation	1/51

Multi-objective optimization approach

Optimization algorithm. The Nondominated Sorting Genetic Algorithm II (NSGA-II) with single point crossover and integer flip mutation operators is used. This is one of the most popular multi-objective optimization algorithms and it is suitable for the procedure proposed.

Parameters tuning. The chromosome length is given by $N+2Np$ (see Figure 3.4). Following the parameter values recommended in Deb et al. (2002), the crossover probability is $p_c = 0.9$ and the mutation probability is $p_m = 1/(N + 2Np)$ (1 divided by the number of decision variables). The number of generations (G) was determined by experimentation.

The NSGA-II algorithm parameters are shown in Table 3.9, and the objective functions are those defined in Section 3.1.2. These functions have to be minimized while satisfying the capacity constraints. A customary way of dealing with constraints in genetic algorithms is penalizing the fitness values when the constraints are not satisfied. When the difference between the capacity of the system and the cooling demand is negative, it is multiplied by a negative factor. This product is added to each objective function in order to worsen the fitness values. The penalty factor should be carefully chosen because larger values may force the algorithm to converge without sufficiently exploring the search space; on the other hand, smaller values may require a greater number of generations.

After preliminary trials, combinations of different levels of "Penalty" and "Generations" were tested. In order to capture the variability of the settings, 10 replicates of each combination were run. The performance measure used to compare the alternatives is the hypervolume indicator which is the volume covered by the elements of a nondominated set, and it is measured relative to a worst possible point in the objective space (see

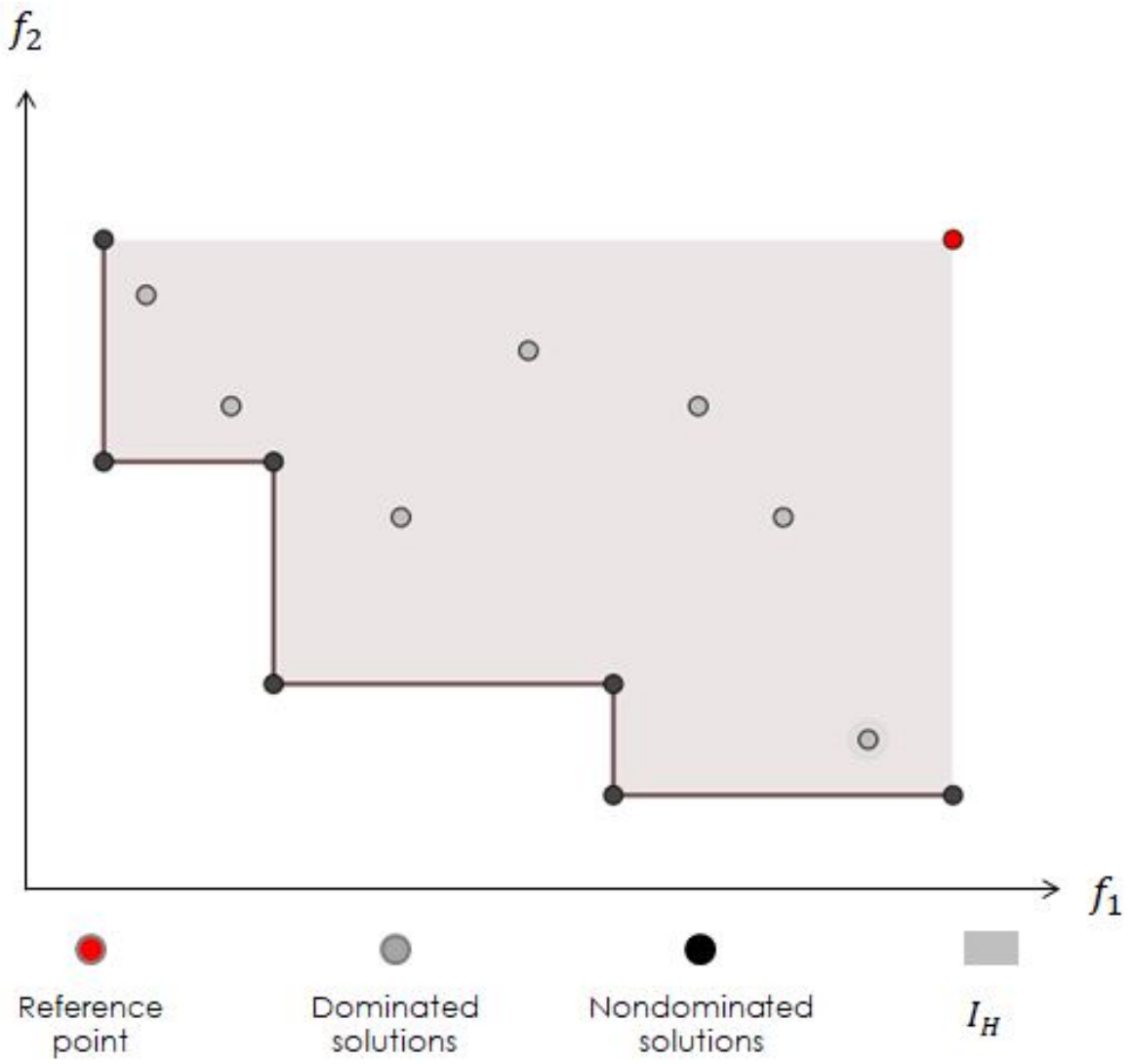

Figure 3.5: Illustration of the hypervolume indicator

Figure 3.5). Let v_i be the volume enclosed by solution $w_i \in W$. Then, a union of all hypercubes is found and its hypervolume (I_H) is calculated (Equation 3.15).

$$I_H(W) = \bigcup_{1}^{|W|} v_i \tag{3.15}$$

If a set W_i has a greater hypervolume than a set W_j, then W_i is taken to be a better set of solutions than W_j. In this work, it is considered the hypervolume difference to a reference set R, defined as in Equation 3.16, where smaller values correspond to higher quality. If the reference set is not given, it is considered $I_H(R) = 0$.

$$I_H^-(W) = I_H(R) - I_H(W) \tag{3.16}$$

The results of the experiment are shown in Figure 3.6. The number of generations was set at 50000 because it can be seen that the hypervolume indicator remains relatively

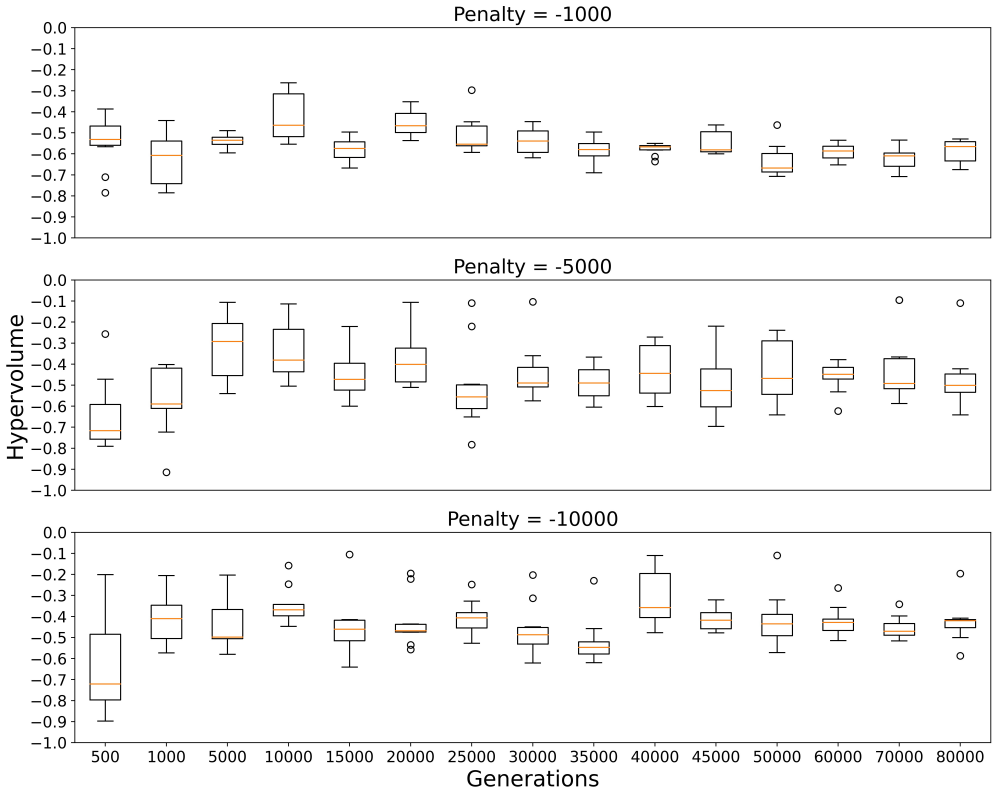

Figure 3.6: Hypervolume results for different values of "Penalty" and "Generations"

stagnant from this point on. The most convenient choice of penalty factor is -1000, since the hypervolume indicator is smaller and shows less variation in comparison with the values obtained when bigger penalties are applied.

Optimization results. In order to compare the procedures, it was considered the case of 3 chillers in the system ($N = 3$). The approximate Pareto fronts obtained in the 10 runs are condensed in the nondominated solutions shown in Figure 3.7. The chiller models and the energy consumption of each nondominated solution are shown in Table 3.10. The corresponding OCL can be seen in Table 3.11. We may observe that initial cost and energy consumption are conflicting objectives. Solution "I" is the most expensive one (843212.4 USD), but it has the lowest energy consumption (4046.3 MWh per year). On the other hand, Solution "A" is the cheapest one (629543.6 USD), but it has the highest energy consumption (4515.2 MWh per year).

The algorithm also produced seven additional solutions to be considered. Solutions "C", "D", "F", "H" and "I" have at least two units of the same model, which means commonality of spare parts. Another well appreciated feature in chiller plants is redundancy. In this case, all the solutions have redundant capacity, and the lowest cost per installed

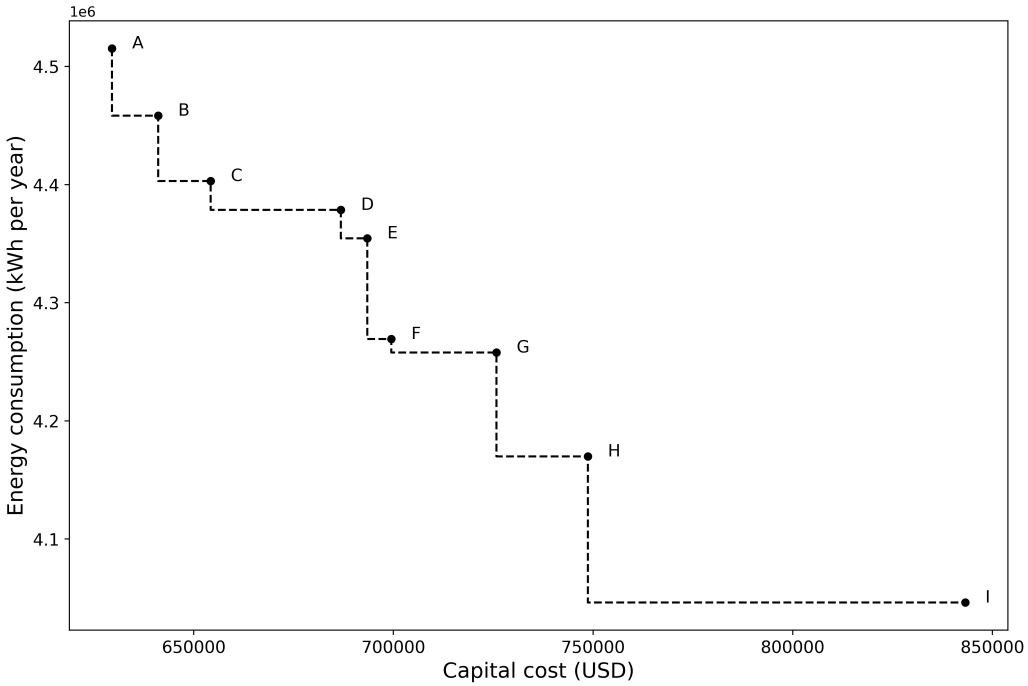

Figure 3.7: Nondominated solutions (Generations: 50000; Penalty: -1000)

Table 3.10: Chiller selection for the nondominated solutions (Generations: 50000; Penalty: -1000)

Solution	Chiller selection	Capital cost(USD)	Energy consumption(kWh per year)
A	1 x 500 TR, 1 x 325 TR and 1 x 275 TR	629543.6	4515196
B	1 x 500 TR, 1 x 325 TR and 1 x 300 TR	641118.8	4458404
C	1 x 500 TR and 2 x 325 TR	654239.6	4403033
D	2 x 500 TR and 1 x 160 TR	686866.8	4378619
E	1 x 500 TR, 1 x 450 TR and 1 x 250 TR	693475.6	4354556
F	2 x 500 TR and 1 x 200 TR	699496	4269284
G	1 x 500 TR, 1 x 450 TR and 1 x 325 TR	725832.4	4257838
H	2 x 500 TR and 1 x 325 TR	748726	4169865
I	3 x 500 TR	843212.4	4046262

Table 3.11: Nondominated solutions (Generations: 50000; Penalty: -1000)

Solution	Model	Partial load ratio (%)								Capital cost (USD)	Energy consumption (kWh per year)
		Level 1	Level 2	Level 3	Level 4	Level 5	Level 6	Level 7	Level 8		
A	500	24	33	59	53	76	64	73	84	629543.6	4515196
	275	0	45	77	53	44	87	95	83		
	325	26	0	23	84	58	71	53	77		
B	500	0	43	76	60	73	85	69	82	641118.8	4458404
	325	31	0	16	70	46	51	76	88		
	300	34	26	51	54	60	68	72	71		
C	500	18	44	56	55	58	68	63	87	654239.6	4403033
	325	33	0	27	80	62	92	74	77		
	325	0	22	68	48	64	49	78	68		
D	500	25	41	28	78	61	62	73	71	686866.8	4378619
	500	0	0	59	40	60	76	68	84		
	160	42	52	87	51	47	54	52	69		
E	250	0	0	82	60	81	78	74	86	693475.6	4354556
	500	21	33	0	46	37	69	57	68		
	450	20	27	80	63	63	51	69	72		
F	200	34	0	46	57	61	73	70	82	699496	4269284
	500	25	19	62	56	58	66	66	77		
	500	0	39	35	56	54	61	64	68		
G	500	25	58	51	44	58	70	60	60	725832.4	4257838
	325	22	0	55	62	47	78	62	81		
	450	0	0	33	57	54	41	65	74		
H	500	25	24	48	50	53	65	59	70	748726	4169865
	325	22	0	26	52	53	48	67	68		
	500	0	34	51	52	50	61	57	65		
I	500	21	34	45	46	40	67	60	56	843212.4	4046262
	500	0	24	42	40	49	41	51	62		
	500	18	0	28	49	47	48	47	60		

capacity is offered by Solution "I". In tight spaces one important decision parameter is the system footprint. This would be a disadvantage of Solution "I" because it is formed by the biggest units. It can be observed in the OCL results (Table 3.11) that the solutions are well balanced in terms of operating time, which means that the units will wear out evenly.

3.1.5 Conclusions

This paper extends current research by incorporating the chiller selection into the typical OCL problem. The results provide the chiller selection and the operation schedule. The outdoor temperature was included as an independent variable in both the capacity functions and the consumption functions. This inclusion caused an increase in the explanatory power of 3% for the capacity functions and of 23% for the consumption functions on average.

In the air-cooled screw chillers analyzed, the consumption is a quadratic function of the PLR, which makes it possible to use an exact algorithm for selecting chillers based on the cost of both the plant and the energy consumption. Moreover, taking advantage of the fact that these functions may also be modeled as linear functions with a difference in explanatory power of only 1% on average, a linear approximation for the MINLP is proposed when the problem is excessively large. It is advantageous because the problem grows exponentially as the number of chillers in the system increases. Problems that take hours or even days to be solved may be solved in a few seconds using this approximation with a relative error of between 3% and 11%.

The mathematical programming approach proposed in this paper provides an exact solution to the chiller selection problem. It uses a single objective function that is a linear combination of the two objectives. The terms of this linear combination are weighted by the depreciation rate and the electricity price, but the latter is not necessarily fixed, which makes this approach less convenient under high variability. Moreover, in the cases where the capital costs and the operating costs are assumed by different agents, combining the two objectives may not be the best alternative. In those situations, the multi-objective optimization of the capital costs and the energy consumption measured in their original units is a better option. This approach produces a set of nondominated solutions that would allow the engineers to conduct a subsequent trade-off analysis. A major takeaway from the case study is that all the solutions have a large installed capacity in relation to the peak load demand, which is far from intuitive solutions and confirms the necessity of a systematic procedure. Finally, it is important to note that this selection scheme may be used with other types of chillers as well as with a vast variety of engineering problems related to equipment selection when the performance functions and the demand profiles are known.

Chapter 4

Application 2

4.1 Article 2: Optimal selection of utility plants in oil and gas offshore platforms

Authors

Luis A. Pargas-Carmona[a], Júlio A. M. Da Silva[a], Ângelo M. O. Sant'Anna[a], Daniel A. Flórez-Orrego[b], Cyro Albuquerque Neto[c], Silvio de Oliveira Junior[b].

(a) Federal University of Bahia - Polytechnic School, R/Prof. Aristides Novis 2, Federação, Salvador (BA) 40210-630, Brazil.

(b) University of São Paulo - Polytechnic School, Av. Prof. Mello Moraes, 2231, Cidade Universitária, Butantã, Sao Paulo (SP) 05508900, Brazil.

(c) University Center FEI—Educational Foundation of Ignatius "Priest Sabóia de Medeiros", Av. Humberto de Alencar Castelo Branco, Assunção, São Paulo (SP) 09850901, Brazil.

Abstract

The utility plants in oil and gas platforms should be designed to meet the electrical demand during the lifetime at minimum cost. A great deal of effort has been devoted to determining the optimal load share of each reciprocating engine/gas turbine operating in parallel that minimizes the overall fuel consumption. However, the selection of the models and the number of units in the system is normally left out of the problem formulation. This paper introduces a procedure to make the optimal selection of utility plants in floating, production, storage and offloading (FPSO) platforms. It is analyzed a case study by using the following two alternative approaches: i) a mono-objective optimization of a single cost-based function and ii) a multi-objective optimization of capital cost and fuel consumption. Under the first approach the fuel consumption is translated into monetary

terms. On the other hand, the multi-objective approach produces a set of nondominated solutions that enables a subsequent engineering analysis. A major takeaway from the case study is that all the solutions obtained are better than the standard solution of three aeroderivative gas turbines model GE LM2500+RD (G4) (with a capital cost of 40.05 Millions of USD and a fuel consumption of 9.999×10^4 TJ at the optimal setting during the lifetime of the system). The results confirm the necessity of a systematic selection procedure.

Keywords: Equipment selection; Floating, Production, Storage and Offloading; Mono-objective optimization; Multi-objective optimization; Oil and gas platforms.

4.1.1 Introduction

The universal demand for processes with lower CO2 emissions has increased the number of papers in the literature on power plant configurations for floating, production, storage and offloading (FPSO) platforms aiming high efficiencies/low emissions. Barbosa et al. (2018) studied the performance of various cogeneration plants on an offshore platform over the lifetime of the field. The cogeneration unit equipped with reciprocating engine showed the lowest variation under time-changing operating conditions and the composition of the well. The steam turbine cycle showed the lowest exergy efficiency over the lifespan. da Silva & de Oliveira Junior (2018) calculated the unit exergetic costs and CO2 emissions of the products of an offshore platform over its lifetime. Three different types of cogeneration plants and two modes of operation of the primary processing plant (total injection or partial gas export) were considered. The reciprocating engine proved to be the most efficient, showing lower unit exergy costs and CO2 emission rates. Nord & Bolland (2013) compared the off-design performance of gas turbine systems and combined cycles intended to operate on offshore platforms. Combined cycles offered 13 p.p. higher energy efficiencies, 60% higher power-to-weight ratios and 25% lower CO2 emissions. These analyses were extended by Riboldi & Nord (2017) to incorporate the effect of variable energy demands over the lifetime, especially during peak production and end-of-life. Also, depending on the heat-to-power ratio demanded by the oil processing, the CO2 emissions could be reduced between 9 and 22%. Nascimento Silva, Flórez-Orrego & de Oliveira Junior (2019) and Nascimento Silva et al. (2020) compared the thermodynamic and environmental performance of various cogeneration systems aimed to operate on FPSOs, ranging from simple cycle gas turbine systems with amine flue gas purification units to complex oxy-combustion cycles. Oxycombustion power cycles allowed a simultaneous increase in power generation efficiency and facilitated the carbon capture process. Flórez-Orrego et al. (2021) developed a systematic method to synthesize the best configuration of floating power generation systems in offshore application using an optimization routine based on the concept of sawtooth plot. The best configuration strongly depended on the

profile of energy demands, the minimum generation capacity and the characteristics of the power generation systems. Later, Flórez-Orrego et al. (2022) performed an optimization process of the dispatch and load distribution among a set of modular power generation systems equipped with carbon capture units to be implemented in the offshore petroleum sector. The integration of carbon capture technologies reportedly required carbon taxes higher than 40 USD/tCO2 to supersede the existing cogeneration systems in offshore platforms. Carranza Sánchez & de Oliveira (2015) concluded that simple cycle gas turbines equipped with carbon capture systems have potential to reduce the CO2 emissions by 77% at the expense of a reduction of only 2.8 p.p on the platform efficiency. Cuchivague (2015) studied the performance of the cogeneration system of an offshore platform operating under three conditions of oil production, considered as representative of the useful life of the field. A combined cycle reportedly allowed to increase the efficiency by 24%, compared to the conventional system, despite the integration of a post-combustion carbon capture unit. Nguyen et al. (2016) presented several alternatives for the mitigation of CO2 emissions in the offshore oil production sector. According to the authors, the improvement of heat recovery systems, carbon capture and, eventually, the electrification of platforms could reduce CO2 emissions by 15%. Some authors studied the low-temperature waste heat recovery from the exhaust gases of gas turbines using organic Rankine cycles in FPSOs. According to Barrera & Sahlit (2013), the use of an ORC cycle would allow a reduction of up to 15% in fuel consumption per barrel of oil. According to Veloso (2015), different fluids can be used depending on the power generation range (1.5 and 6.3 MW) and the total area of the ORC cycle. Pierobon et al. (2013) developed a multi-objective optimization considering efficiency, volume and investment of ORC cycles for its application in offshore platforms. Their results suggest acetone (27% efficiency, NPV 17.7 MUSD) and cyclopentane (28.1% efficiency, NPV 20.1 MUSD) as optimal working fluids. The combined use of ORCs and absorption chillers were also proposed as potential improvements in the cogeneration plants of the platforms (BARRERA; SAHLIT, 2013). Reis & Gallo (2018) and Reis, Guillen & Gallo (2019) optimized the over-time performance of an ORC coupled to a conventional gas turbine system on an offshore platform. The ORC cycle contributed up to 20% of the total electricity generated by the utility system, increased the efficiency of the cogeneration system by 11 p.p (up to 55.8%) and reduced total CO2 emissions by up to 22%.

Among the most common optimization techniques applied to thermal plants are the genetic and evolutionary algorithms. These algorithms are usually used with multi-objective energy, economic or environmental functions. Some works aimed to obtain design parameters such as temperatures, pressures, and efficiencies for combined cycle power plants by genetic algorithm (AHMADI; DINCER; ROSEN, 2011; AHMADI; DINCER, 2011a) or NSGA-II (AHMADI; DINCER, 2011b). Shamoushaki Farrokh Ghanatir & Ahmadi (2017) found that NSGA-II achieves more optimized results than MOPSO and MOEA-

D for a gas turbine cycle study case. Other works aimed to define the design variables and layout of combined cycle heat recovery steam generator, applying genetic algorithm (MOHAGHEGHI; SHAYEGAN, 2009; REZAIE; TSATSARONIS; HELLWIG, 2019) or NSGA-II (SAYYAADI; MEHRABIPOUR, 2012). Rovira et al. (2011) determined the combined cycle design parameters including the choice of one to three turbines with different powers using a genetic algorithm. Considering the availability of 4 gas turbine models from different manufacturers, Cao et al. (2017) analyzed a gas turbine and cascate CO2 combined cycle, also with genetic algorithm optimization. Some works included the choice between several pre-defined plants in their optimization, as Njoku et al. (2020), who considered 19 configurations of combined power plants using multicriteria decision analysis, and Wilding, Murray & Memmott (2020), who tested 22 configurations of nuclear power plants with NSGA. To not depend on a predetermined configuration, Koch, Cziesla & Tsatsaronis (2007) proposed the solution of a generic superstructure for power plant combined cycles with a database of gas turbines available in the market. They applied the model to optimize the configuration of a case study with an evolutionary algorithm. The superstructure concept was also used by Wang et al. (2015) to find the multi-stage configuration of steam cycle power plants with an evolutionary algorithm. Using different approaches in the optimization procedure is also a common practice in this field. For instance, Allahyarzadeh-Bidgoli et al. (2021) used both NSGA-II and a gradient-based method to minimize the total fuel consumption in a FPSO platform.

Even though there is a vast literature on adjusting the load distribution of existing reciprocating engines and gas turbines in FPSO applications, the equipment selection is not conceived as an optimization problem. This paper introduces a procedure to make the optimal selection of utility plants in FPSO platforms by using the following two alternative approaches: i) a mono-objective optimization of a single cost-based function and ii) a multi-objective optimization of capital cost and power consumption. The novelty of this work is to combine the loading problem and the selection problem into a single formulation.

4.1.2 FPSO utility plants

A typical utility plant for FPSO platforms operating in pre-salt fields (Figure 4.1) is composed of four gas turbines (GT) of about 25 MWe each and a waste heat recovery unit (WHRU). One of the gas turbines is kept in stand-by mode while the others are started according to the demand. The WHRU is used to heat water from approximately 110^{o}C to 130^{o}C using a fraction of the energy present in the exhausting gases. While the main consumer of power are the compression trains used for natural gas compression, injection and transportation, the main consumer of heat is the petroleum primary separation into oil, gas and water which uses heat to warm-up the petroleum and the dilution water used

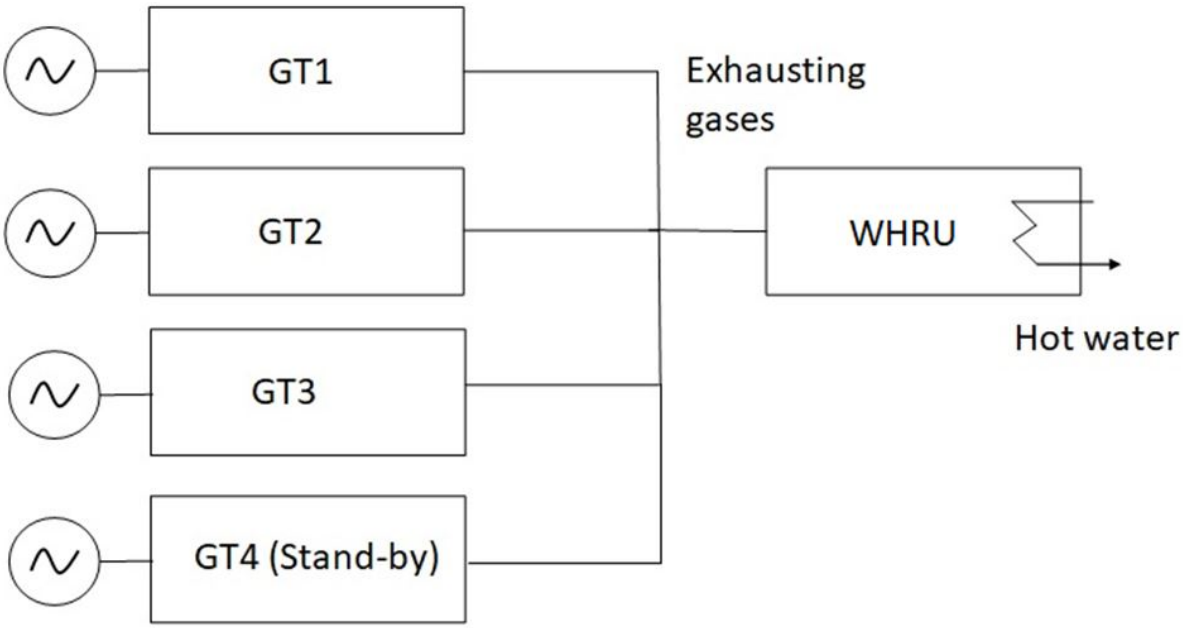

Figure 4.1: Typical utility plant for FPSO platforms operating in pre-salt fields

in the separation.

Since the variation in exhausting gases temperature (about 550^{o}C) and power (about 150 MWt) by different selections of GT/ reciprocating engines is not enough to jeopardize the supply of energy required by the WHRU (25 MWt at project point), the hot water demand will be disregarded during selection and operation optimization of power generating equipment.

4.1.3 Optimization procedure

The main processes present in an FPSO platform are: the primary separation of oil, gas and water; gas compression; gas separation using membranes; and water and oil pumping. A utility plant composed of four aeroderivative gas turbines (3 + 1 in standby) is the standard selection to supply the required electricity and the heat (from exhausting gases) for the processes.

The problem considers C engine/turbine models available for purchase and N units to be selected. Both the electrical demand and the efficiency functions of the models available are known, and the system is required to operate in a span of P years to satisfy the electrical demand (d_j) of each year j at minimum cost. In the selection procedure depicted in Figure 4.2, the engine/turbine selection and the corresponding load distribution for all the years are obtained when the optimization algorithm produce a feasible solution.

The efficiency of an engine/turbine i (η_i) is a function of the partial load (R), which is the actual power generated by the unit divided by its full power. Modeling this function requires empirical data, and it can be estimated by a quadratic model (Equation 4.1)

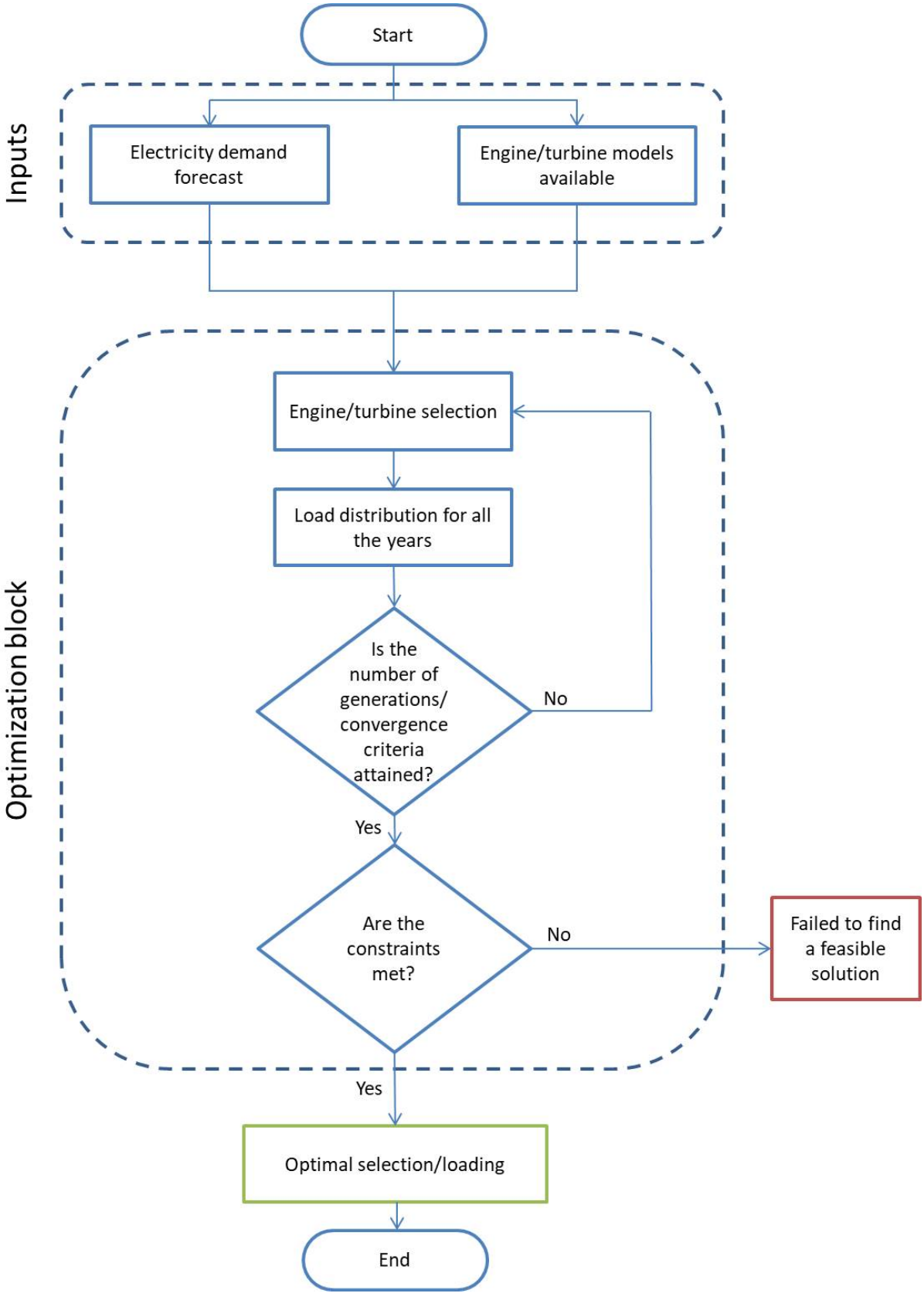

Figure 4.2: General flowchart of the optimization procedure

when the local temperature variation is small, which is the case of the Brazilian pre-salt region.

$$\eta_i = \beta_{1i} \cdot R^2 + \beta_{2i} \cdot R + \beta_{3i} \tag{4.1}$$

Given the full power of each engine/turbine k selected with the model i (q_i), the power required by the units selected operating at the configuration scheduled for year j (g_j) is obtained from Equation 4.2.

$$g_j = \sum_{i=1}^{C} \sum_{k=1}^{N} \frac{q_i \cdot R_{ijk}}{\beta_{1i} \cdot R_{ijk}^2 + \beta_{2i} \cdot R_{ijk} + \beta_{3i}} \tag{4.2}$$

The total power generated at year j (h_j) is calculated by Equation 4.3.

$$h_j = \sum_{i=1}^{C} \sum_{k=1}^{N} q_i \cdot R_{ijk} \tag{4.3}$$

In this section are presented two alternative formulations for the selection problem. The first alternative is a mono-objective optimization of a single cost-based function, and the other is a multi-objective optimization of capital costs and fuel consumption.

Mono-objective optimization approach

It is possible to obtain a combined objective function (Equation 4.4) by summing up the operating cost and the capital cost. The first term of Equation 4.4 is the operating cost, which is calculated as the present value (at a discount rate r) of the power required at each year (g_j) multiplied by both the fuel price (w) and the operating hours per year (t_j). The second term of Equation 4.4 is the capital cost, which is the sum of the cost (c_i) of each engine/turbine selected. The selection binary variable S_{ik} assumes the value of 1 when the model i is selected for engine/turbine k, and 0 otherwise.

$$\text{Objective value} = \sum_{j=1}^{P} \frac{w \cdot t_j \cdot g_j}{(1+r)^j} + \sum_{i=1}^{C} \sum_{k=1}^{N} S_{ik} \cdot c_i \tag{4.4}$$

The feasible region is defined by a set of constraints. Equation 4.5 establishes that there is one engine/turbine model for each unit selected. This does not prevent the units selected from having the same model.

$$\sum_{i=1}^{C} S_{ik} = 1 \tag{4.5}$$

The load ratio (R_{ijk}) can take on any value from a minimum specified by the manufacturer (m_i) to 1 (Equation 4.6).

$$m_i \leq R_{ijk} \leq 1 \tag{4.6}$$

Equation 4.7 guarantees that the load ratio will be zero when the unit is not selected.

$$R_{ijk} \leq S_{ik} \tag{4.7}$$

Equation 4.8 guarantees that the electrical demand (d_j) will be satisfied by the capacity at each year (h_j).

$$h_j \geq d_j \tag{4.8}$$

Multi-objective optimization approach

Combining the capital costs and the power consumption in a single objective function is not always the best choice because it requires both objectives to be expressed in monetary terms, and the operating costs depend on highly variable prices. On the other hand, under a multi-objective optimization approach the fuel consumption is not required to be measured in monetary terms. The first objective is the sum of the total fuel consumption of the engines/turbines selected. The second objective is the capital cost measured as the sum of the cost of the engines/turbines selected.

The load ratio (R_{ijk}) can take on any value from a minimum specified by the manufacturer (m_i) to 100%, i.e. the operating range of unit i is $\{0\} \bigcup [m_i; 1]$. Since this is not a valid variable range in many multi-objective optimization algorithms, a power status variable (P_{ijk}) was included. Thus, in a multi-objective genetic algorithm the chromosome length would be $CN + 2CNP$ (Table 4.1). The population size may be 100, the mutation probability may be $1/(CN + 2CNP)$ (1 divided by the number of variables), and the number of generations may be determined by preliminary trials for each specific configuration.

Table 4.1: Chromosome specification

Selection binary variables					**Power status binary variables**					**Partial load variables**				
S_{11}	...	S_{ik}	...	S_{CN}	P_{111}	...	P_{ijk}	...	P_{CPN}	R_{111}	...	R_{ijk}	...	R_{CPN}

4.1.4 Results

The problem analyzed is the case study presented by Barbosa et al. (2018). The forecasted electrical demand for a period of 22 years is shown in Figure 4.3(a). The corresponding histogram of the electrical demand with a probability density estimation is plotted in Figure 4.3(b).

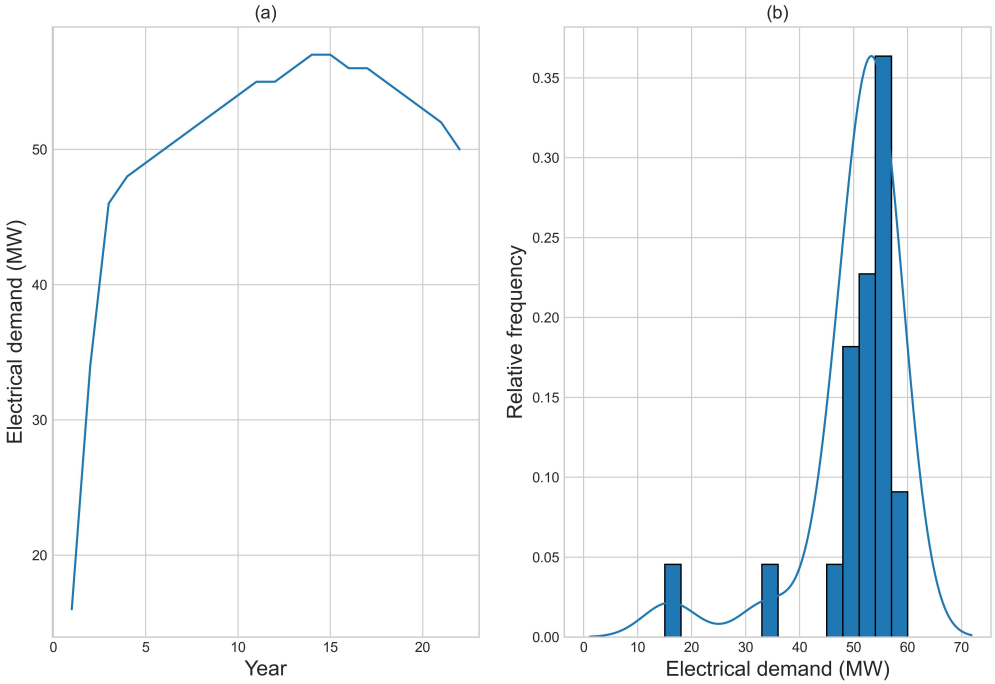

Figure 4.3: Electrical demand profile

The cost and power data of both the reciprocating engine models and the gas turbine models available were obtained from THERMOFLOW Inc. (2021) (Table 4.2). The efficiency curves that can be seen in Figure 4.4 were plotted using the data obtained from Thermoflow Inc. (THERMOFLOW Inc., 2021). The corresponding Ordinary Least Square (OLS) regression parameters β_{1i}, β_{2i} and β_{3i} are shown in Table 4.3.

Table 4.2: Nominal power and cost of the reciprocating engine and gas turbine models available

Unit model	**Unit type**	**Nominal power (kW)**	**Cost (Millions of USD)**
WAR 18V34SGA2	Reciprocating engine	5732	2.83
WAR 20V34SG	Reciprocating engine	9341	3.71
WAR 18V50SG	Reciprocating engine	18759	8.64
GE LM2500+RD (G4)	Gas turbine	33578	13.35
GE LM6000PG	Gas turbine	51678	18.47
Solar Mars 100-T16000S	Gas turbine	11350	6.49
Sol Titan 130-T20500	Gas turbine	10226	7.98
Sol Titan 250-30000S	Gas turbine	21750	9.92
GE LMS100PA	Gas turbine	106300	37.57

The analysis was made for different configurations: i) 3 units (all models), ii) 4 units (all models), iii) 5 units (all models), iv) 3 units (only turbines), and v) 3 units (turbine model GE LM2500+RD (G4)), which is the standard selection for this sort of application.

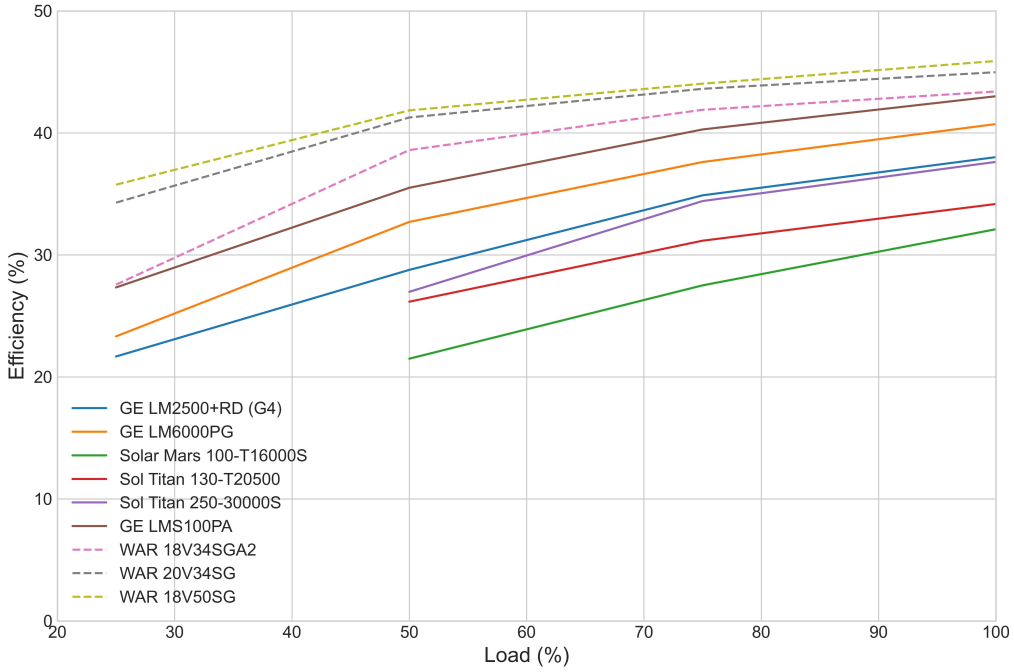

Figure 4.4: Efficiency curves of the reciprocating engine and gas turbine models available

The discount rate used in the optimization problem was 13.05%, which is the mean value in the period 2016-2020 for capital cost in the oil/gas (production and exploration) industry for emerging markets according to Damodaran, Aswath (2021). The fuel (natural gas) cost considered was 2.77 USD per Million BTU (2.63 USD per GJ), which is the mean value for the Henry Hub Natural Gas Spot Price in the period 2016-2020 (U.S. Energy Information Administration (EIA), 2021).

Since several engineering and economic constraints are not explicitly taken into consideration, the problem was formulated for different combinations of models available (e.g. turbines only or all engines/turbines) and different number of units in the system. The mono-objective problems were submitted to NEOS Server (Czyzyk; Mesnier; Moré, 1998; Dolan, 2001; Gropp; Moré, 1997) in AMPL format (FOURER, 1996) and they were solved using BARON, which is a mathematical optimization software for mixed integer nonlinearly constrained problems (TAWARMALANI; SAHINIDIS, 2005; SAHINIDIS, 2017). On the other hand, the multi-objective optimization problems were solved with the Nondominated Sorting Genetic Algorithm (NSGA-II) using jMetalPy, which is an object-oriented Python-based framework for multi-objective optimization with metaheuristic techniques (BENíTEZ-HIDALGO et al., 2019).

Table 4.3: Regression parameters of the efficiency functions

Unit model	OLS Parameters		
	β_{1i}	β_{2i}	β_{3i}
WAR 18V34SGA2	-0.3812	0.6797	0.1326
WAR 20V34SG	-0.2248	0.4187	0.2541
WAR 18V50SG	-0.1692	0.3419	0.2845
GE LM2500+RD (G4)	-0.1588	0.4190	0.1210
GE LM6000PG	-0.2508	0.5419	0.1148
Solar Mars 100-T16000S	-0.1128	0.3814	0.0525
Sol Titan 130-T20500	-0.1592	0.3990	0.1020
Sol Titan 250-30000S	-0.3384	0.7206	-0.0059
GE LMS100PA	-0.2180	0.4797	0.1678

Mono-objective optimization results

The results for the mono-objective problems are summarized in Table 4.4. The capital cost of the optimal selections ranges from 24.49 Millions of USD to 31.45 Millions of USD, and the fuel consumption ranges from 7.76×10^4 TJ to 9.25×10^4 TJ. The standard selection of three GE LM2500+RD (G4) units was included in the analysis in order to determine the optimal loading and the corresponding fuel consumption. All the results obtained are superior to the standard selection at its optimal setting in both capital cost and fuel consumption.

Table 4.4: Optimal selection for different configurations (mono-objective optimization approach)

Number of units	Models available	Optimal selection	Capital cost (Millions of USD)	Fuel consumption (TJ)
3	All Engines/Turbines	1 x Sol Titan 250-30000S 2 x WAR 18V50SG	27.21	8.36×10^4
4	All Engines/Turbines	3 x WAR 20V34SG 1 x GE LM2500+RD (G4)	24.49	8.78×10^4
5	All Engines/Turbines	1 x WAR 20V34SG 2 x WAR 18V34SGA2 2 x WAR 18V50SG	26.67	7.76×10^4
3	All Turbines	1 x GE LM6000PG 2 x Solar Mars 100-T16000S	31.45	9.25×10^4
3	Standard selection	3 x GE LM2500+RD (G4)	40.05	9.999×10^4

In order to assess the effect of the variations of both the discount rate (mean: 13.05%; standard deviation: 2.29%) and the fuel (natural gas) price (mean: 2.77 USD per Million BTU; standard deviation: 0.28 USD per Million BTU), the objective value was recalculated for each combination of r and w plus or minus two standard deviations. The objective value and its corresponding variation range for each configuration at the optimal loading is shown in Figure 4.5.

The partial ratios for the optimal selections under the mono-objective approach are shown in Table 4.5. There is no indication that the units have to start sequentially after

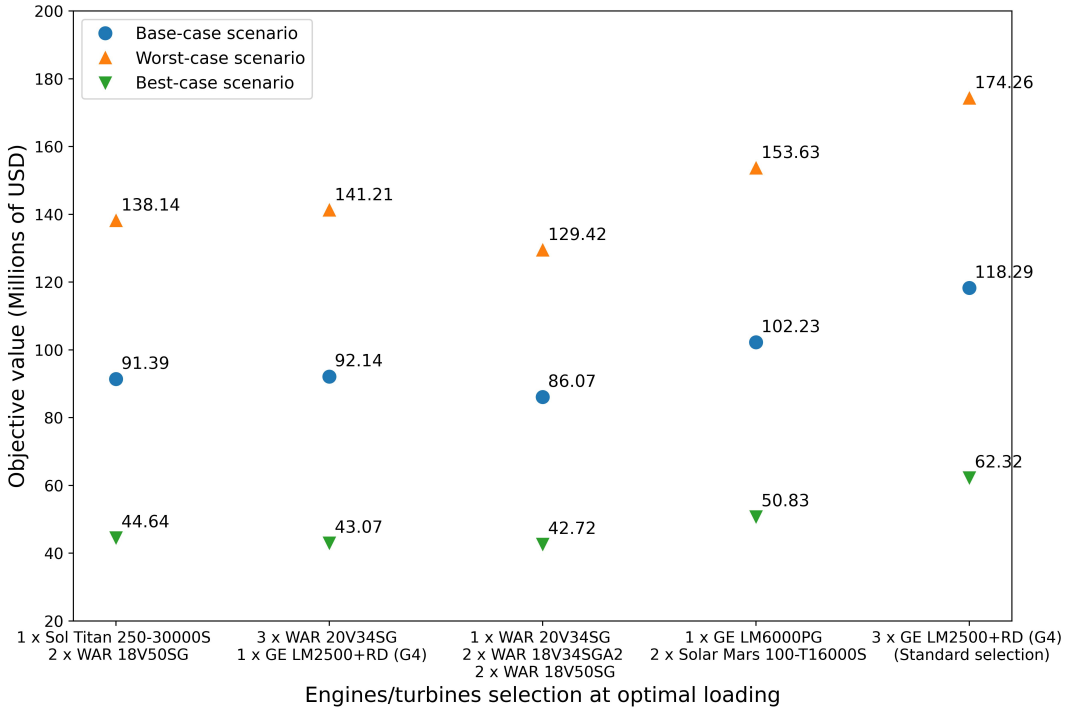

Figure 4.5: Objective value variation range (mono-objective optimization approach)

other units operate at full capacity. On the contrary, it can be seen that the units in the standard selection seldom operate at a load of 100%.

Multi-objective optimization results

After preliminary trials it was noticed that, beyond a certain extent, increasing the number of generations in the NSGA-II does not lead to better solutions. Based on that, one problem was formulated for turbines only and 30000 generations. Likewise, a second problem was formulated for all the engines/turbines models available and 50000 generations. The approximate Pareto fronts of these problems are shown in Figure 4.6. There is one point of the turbines front not dominated by the solutions of the engines/turbines front. Notwithstanding, the nondominated solutions were integrated in a single front.

The selections for the nondominated solutions are shown in Table 4.6. The multi-objective approach enables the possibility of producing nondominated solutions with the same number of units. For instance, solutions B, C and D are different selections with 4 engines/turbines.

It is important to note that the standard selection of three GE LM2500+RD (G4) units (with a capital cost of 40.05 Millions of USD and a fuel consumption of 9.999×10^4 TJ at its optimal setting) is dominated by Solutions A, B, C and D. Even Solution E is better than the standard selection in terms of fuel consumption (Figure 4.7).

Table 4.5: Optimal load ratios for the mono-objective optimization problem

Selection	Year																					
	1	**2**	**3**	**4**	**5**	**6**	**7**	**8**	**9**	**10**	**11**	**12**	**13**	**14**	**15**	**16**	**17**	**18**	**19**	**20**	**21**	**22**
Sol Titan 250-30000S	0.00	0.89	0.88	0.88	0.89	0.89	0.90	0.91	0.91	0.92	0.93	0.93	0.94	0.94	0.94	0.94	0.94	0.93	0.92	0.91	0.91	0.89
WAR 18V50SG	0.85	0.78	0.72	0.77	0.79	0.81	0.84	0.86	0.88	0.91	0.93	0.93	0.95	0.97	0.97	0.95	0.95	0.93	0.91	0.88	0.86	0.81
WAR 18V50SG	0.00	0.00	0.72	0.77	0.79	0.81	0.84	0.86	0.88	0.91	0.93	0.93	0.95	0.97	0.97	0.95	0.95	0.93	0.91	0.88	0.86	0.81
WAR 20V34SG	0.73	0.25	0.25	0.59	0.62	0.64	0.67	0.69	0.71	0.73	0.76	0.76	0.80	0.84	0.84	0.80	0.80	0.76	0.73	0.71	0.69	0.64
WAR 20V34SG	0.25	0.25	0.25	0.59	0.62	0.64	0.67	0.69	0.71	0.73	0.76	0.76	0.80	0.84	0.84	0.80	0.80	0.76	0.73	0.71	0.69	0.64
WAR 20V34SG	0.73	0.00	0.83	0.59	0.62	0.64	0.67	0.69	0.71	0.73	0.76	0.76	0.80	0.84	0.84	0.80	0.80	0.76	0.73	0.71	0.69	0.64
GE LM2500+RD (G4)	0.00	0.87	1.00	0.94	0.94	0.95	0.96	0.98	0.99	1.00	1.00	1.00	1.00	1.00	1.00	1.00	1.00	1.00	1.00	0.99	0.98	0.95
WAR 20V34SG	0.00	0.82	0.82	0.85	0.79	0.81	0.83	0.84	0.86	0.87	0.89	0.89	0.92	0.98	0.98	0.92	0.92	0.89	0.87	0.86	0.84	0.81
WAR 18V34SGA2	0.00	0.81	0.81	0.00	0.79	0.80	0.81	0.82	0.83	0.84	0.85	0.85	0.86	0.90	0.90	0.86	0.86	0.85	0.84	0.83	0.82	0.80
WAR 18V50SG	0.85	0.25	0.90	0.94	0.87	0.89	0.91	0.93	0.95	0.97	0.99	0.99	1.00	1.00	1.00	1.00	1.00	0.99	0.97	0.95	0.93	0.89
WAR 18V50SG	0.00	0.90	0.90	0.94	0.87	0.89	0.91	0.93	0.95	0.97	0.99	0.99	1.00	1.00	1.00	1.00	1.00	0.99	0.97	0.95	0.93	0.89
WAR 18V34SGA2	0.00	0.00	0.00	0.83	0.79	0.80	0.81	0.82	0.83	0.84	0.85	0.85	0.86	0.90	0.90	0.86	0.86	0.85	0.84	0.83	0.82	0.80
Solar Mars 100-T16000S	0.00	0.00	0.00	0.00	0.00	0.00	0.00	0.00	0.00	0.00	1.00	1.00	1.00	0.00	0.00	0.00	0.00	0.00	1.00	0.00	1.00	0.00
GE LM6000PG	0.31	0.66	0.89	0.93	0.95	0.97	0.99	0.79	0.81	0.83	0.84	0.84	0.86	0.88	0.88	0.86	0.86	0.84	0.83	0.81	0.79	0.97
Solar Mars 100-T16000S	0.00	0.00	0.00	0.00	0.00	0.00	0.00	1.00	1.00	1.00	0.00	0.00	0.00	1.00	1.00	1.00	1.00	1.00	0.00	1.00	0.00	0.00
GE LM2500+RD (G4)	0.48	0.25	0.00	0.43	0.00	0.00	0.00	0.00	0.00	0.80	0.00	0.00	0.00	0.00	0.85	0.00	0.83	0.00	0.00	0.79	0.77	0.00
GE LM2500+RD (G4)	0.00	0.00	0.37	1.00	0.46	0.74	0.76	0.77	0.79	0.80	0.82	0.82	0.83	0.85	0.00	0.83	0.00	0.82	0.80	0.79	0.77	0.74
GE LM2500+RD (G4)	0.00	0.76	1.00	0.00	1.00	0.74	0.76	0.77	0.79	0.00	0.82	0.82	0.83	0.85	0.85	0.83	0.83	0.82	0.80	0.00	0.00	0.74

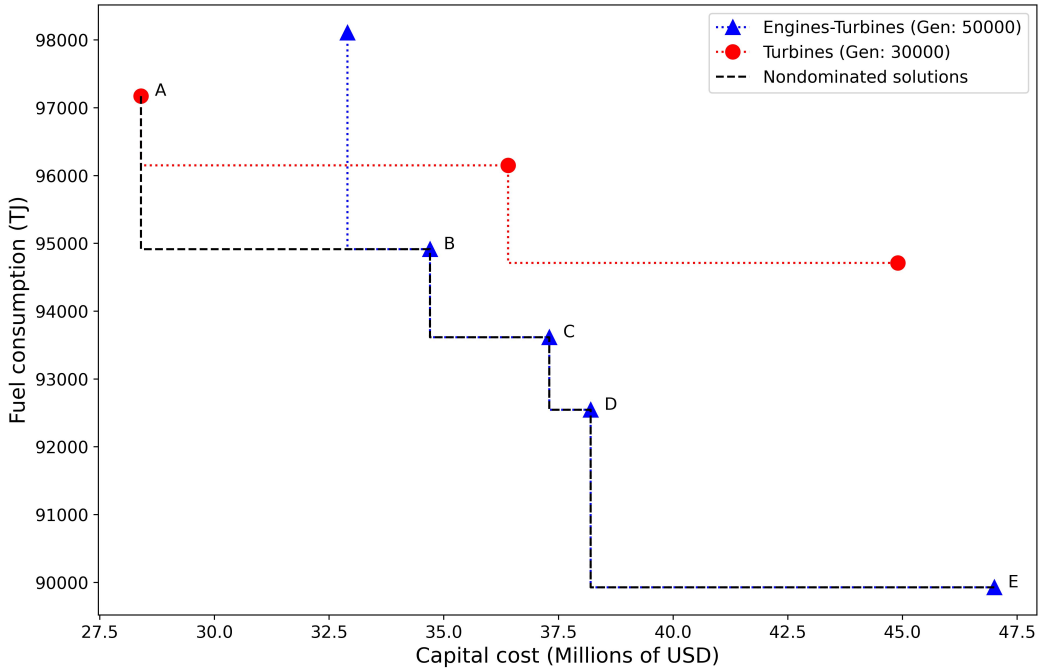

Figure 4.6: Approximate fronts and nondominated solutions (multi-objective approach)

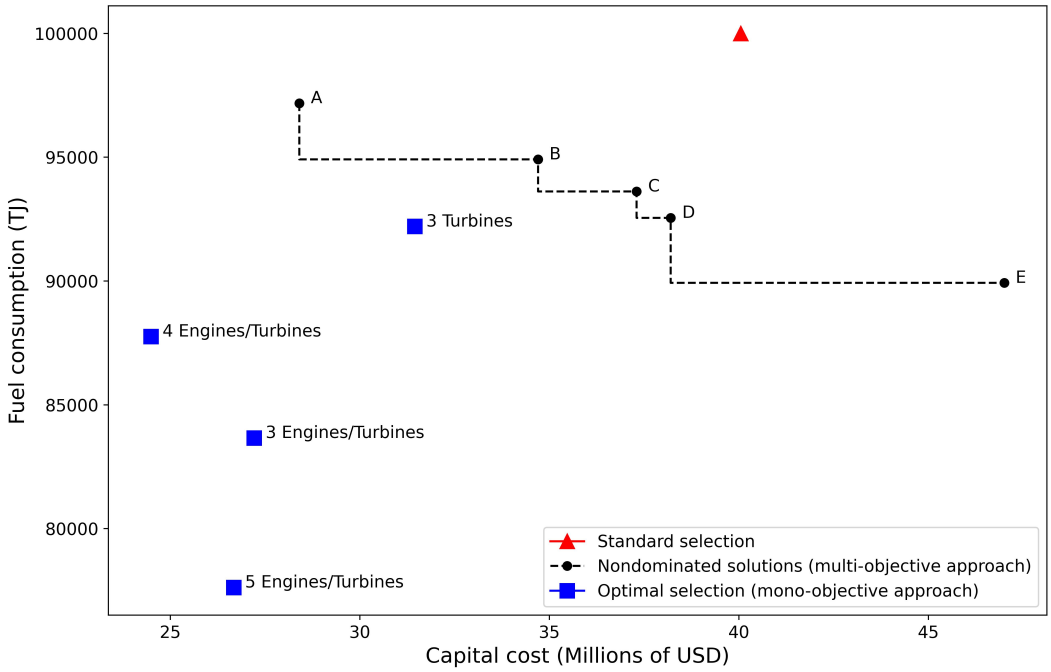

Figure 4.7: Standard selection and optimization results

Table 4.6: Standard selection and nondominated solutions (multi-objective optimization approach)

Solution	Selection	Cost (Millions of USD)	Fuel consumption (TJ)
A	1 x GE LM6000PG 1 x Sol Titan 250-30000S	28.39	9.72×10^4
B	1 x WAR 18V34SGA2 1 x WAR 18V50SG 1 x GE LM2500+RD (G4) 1 x Sol Titan 250-30000S	34.75	9.49×10^4
C	1 x WAR 20V34SG 1 x WAR 18V50SG 1 x GE LM6000PG 1 x Solar Mars 100-T16000S	37.32	9.36×10^4
D	1 x WAR 20V34SG 1 x GE LM6000PG 2 x Sol Titan 130-T20500	38.15	9.25×10^4
E	1 x WAR 18V34SGA2 1 x WAR 20V34SG 1 x WAR 18V50SG 1 x GE LM2500+RD (G4) 1 x GE LM6000PG	47.01	8.99×10^4
Standard selection	3 x GE LM2500+RD (G4)	40.05	9.999×10^4

The optimal load ratios for the nondominated solutions are shown in Table 4.7. It can be seen that some of the units selected are turned off most of the time. This implies redundant capacity, which is desirable but not always affordable.

4.1.5 Conclusions

This paper presented a formal procedure for designing and optimizing utility plants in offshore platforms. The formulation proposed incorporates the equipment selection into the optimal loading problem, which consists of determining the load share of each reciprocating engine/gas turbine operating in parallel that minimizes the overall fuel consumption in the system. Thus, the results provide the selection of the units as well as the corresponding operation schedule. Two alternative formulations of the optimization problem were considered. First, a mono-objective optimization of a single cost-based function. Second, a multi-objective optimization of capital cost and fuel consumption. An important advantage of the latter approach is that it is not necessary to translate the fuel consumption into monetary terms. Instead, it is produced a set of nondominated solutions that can be used in a subsequent trade-off analysis.

The case study consisted of a FPSO platform with a forecasted electrical demand over 22 years. Different technologies such as reciprocating engines and gas turbines were taken into account, and the performance functions of the models available were estimated using the data provided by the manufacturer. The standard selection in FPSO platforms is a utility plant composed of three identical aeroderivative gas turbines plus one standby unit.

Table 4.7: Optimal load ratios for the nondominated solutions

Solution	Selection	Year																					
		1	**2**	**3**	**4**	**5**	**6**	**7**	**8**	**9**	**10**	**11**	**12**	**13**	**14**	**15**	**16**	**17**	**18**	**19**	**20**	**21**	**22**
A	GE LM6000PG	0.32	0.66	0.90	0.95	0.97	0.97	0.71	0.96	0.99	0.78	0.68	0.68	0.89	0.91	0.91	0.89	0.89	0.68	0.78	0.99	0.96	0.97
	Sol Titan 250-30000S	0.00	0.00	0.00	0.00	0.00	0.00	0.66	0.25	0.41	0.65	0.92	0.92	0.47	0.46	0.46	0.47	0.47	0.92	0.65	0.41	0.25	0.00
B	WAR 18V34SGA2	0.00	0.88	0.00	0.00	0.00	0.00	0.00	0.25	0.00	0.00	0.92	0.92	0.95	0.00	0.00	0.95	0.95	0.92	0.00	0.00	0.25	0.00
	WAR 18V50SG	0.00	0.00	0.00	0.00	0.00	0.00	0.34	0.00	0.00	0.25	0.00	0.00	0.00	0.54	0.54	0.00	0.00	0.00	0.25	0.00	0.00	0.00
	GE LM2500+RD (G4)	0.00	0.87	0.74	0.99	0.84	0.87	0.69	0.88	0.98	0.99	0.86	0.86	0.95	0.99	0.99	0.95	0.95	0.86	0.99	0.98	0.88	0.87
	Sol Titan 250-30000S	0.74	0.00	0.98	0.68	0.96	0.96	0.99	0.97	0.93	0.74	0.96	0.96	0.86	0.63	0.63	0.86	0.86	0.96	0.74	0.93	0.97	0.96
C	WAR 20V34SG	0.00	0.00	0.00	0.00	0.00	0.00	0.00	0.00	0.00	0.00	0.42	0.42	0.00	0.00	0.00	0.00	0.00	0.42	0.00	0.00	0.00	0.00
	WAR 18V50SG	0.00	0.00	0.00	0.00	0.00	0.00	0.00	0.00	0.00	0.53	0.00	0.00	0.00	0.00	0.00	0.00	0.00	0.00	0.53	0.00	0.00	0.00
	GE LM6000PG	0.25	0.66	0.79	0.88	0.74	0.97	0.93	0.88	0.92	0.86	0.99	0.99	0.88	0.99	0.99	0.88	0.88	0.99	0.86	0.92	0.88	0.97
	Solar Mars 100-T16000S	0.28	0.00	0.46	0.25	0.98	0.00	0.26	0.59	0.50	0.00	0.00	0.00	0.93	0.55	0.55	0.93	0.93	0.00	0.00	0.50	0.59	0.00
D	WAR 20V34SG	0.00	0.25	0.00	0.00	0.00	0.60	0.00	0.00	0.00	0.00	0.00	0.00	0.00	0.63	0.63	0.00	0.00	0.00	0.00	0.00	0.00	0.60
	GE LM6000PG	0.32	0.62	0.90	0.70	0.79	0.86	0.99	0.98	0.93	0.99	0.75	0.75	0.96	0.99	0.99	0.96	0.96	0.75	0.99	0.93	0.98	0.86
	Sol Titan 130-T20500	0.00	0.00	0.00	0.59	0.80	0.00	0.00	0.25	0.49	0.28	0.72	0.72	0.63	0.00	0.00	0.63	0.63	0.72	0.28	0.49	0.25	0.00
	Sol Titan 130-T20500	0.00	0.00	0.00	0.57	0.00	0.00	0.00	0.00	0.00	0.00	0.87	0.87	0.00	0.00	0.00	0.00	0.00	0.87	0.00	0.00	0.00	0.00
E	WAR 18V34SGA2	0.00	0.00	0.00	0.90	0.00	0.00	0.97	0.00	0.89	0.00	0.55	0.55	0.00	0.00	0.00	0.00	0.00	0.55	0.00	0.89	0.00	0.00
	WAR 20V34SG	0.00	0.00	0.00	0.00	0.00	0.00	0.99	0.00	0.87	0.99	0.73	0.73	0.55	0.92	0.92	0.55	0.55	0.73	0.99	0.87	0.00	0.00
	WAR 18V50SG	0.86	0.00	0.00	0.00	0.88	0.00	0.25	0.90	0.00	0.00	0.72	0.72	0.00	0.00	0.00	0.00	0.00	0.72	0.00	0.00	0.90	0.00
	GE LM2500+RD (G4)	0.00	0.00	0.00	0.00	0.00	0.39	0.94	0.00	0.00	0.00	0.00	0.00	0.00	0.00	0.00	0.00	0.00	0.00	0.00	0.00	0.00	0.39
	GE LM6000PG	0.00	0.66	0.90	0.83	0.63	0.72	0.00	0.68	0.77	0.87	0.61	0.61	0.99	0.94	0.94	0.99	0.99	0.61	0.87	0.77	0.68	0.72

In this case, the selection would be a set of three gas turbines model GE LM2500+RD (G4) with a capital cost of 40.05 Millions of USD and a fuel consumption of 9.999×10^4 TJ. The results of the mono-objective optimization approach showed that this is not the optimal selection even considering gas turbines only (Table 4.4). Likewise, the standard selection is not better than the nondominated solutions produced by the multi-objective approach (Table 4.6). In fact, it is worse than all of them in terms of fuel consumption, which is remarkable considering that the comparison is made with the standard selection at its optimal setting.

Using an evolutionary algorithm is a practical alternative to solve heavily complex problems, but running the same model may yield different solutions and there is no guarantee of finding a global optimum. As it is shown in Figure 4.7, the optimal selections produced by the mixed integer nonlinear program solver in the mono-objective approach for 4 engines/turbines are better than the selections for 4 engines/turbines produced by the NSGA-II algorithm (solutions B, C and D). However, it would be unfair to proclaim the superiority of the mono-objective approach because these solutions were obtained from a smaller search space.

A counterintuitive fact about the results is that some of the units selected are turned off most of the time. Actually, the nondominated solution with the lowest fuel consumption (Solution E) is composed of five units with high percentage of idle time (Appendix 4.7). Having a large installed capacity entails an increase in capital cost, but it may eliminate the necessity of standby units. There are other design criteria such as redundancy, commonality of spare parts, maintenance strategy, and others that are not considered in the problem formulation. The results of the procedure proposed in this paper constitute a solid starting point for further technical analysis. Finally, it is important to note that this selection procedure may also be applied in other engineering contexts as long as both the performance functions and demand profiles are known.

Notation

Subscripts

i: engine/turbine model

j: year

k: engine/turbine in the system

Parameters

β_{1i}, β_{2i} and β_{3i}: efficiency function parameters for engine/turbine model i

C: number of engine/turbine models available

c_i: initial cost of engine/turbine model i

d_j: electrical demand at year j

t_j: operating hours at year j

N: number of engine/turbine in the system

P: number of years

r: interest rate

q_i: full capacity of engine/turbine model i

w: fuel cost

m_i: lower partial load limit of engine/turbine model i

Variables

g_j: power required by the system at year j

h_j: capacity at year j

R_{ijk}: partial load

S_{ik}: selection binary variable (1:"Selected", 0: "Not selected")

P_{ijk}: power status binary variable (1:"On", 0: "Off")

Chapter 5

Final considerations

The selection procedure proposed in this thesis combines the optimal selection problem and the optimal loading problem into a single formulation. Thus, the results provide the selection of the units as well as the corresponding operation schedule. Selecting the units from a set of models available instead of having the units previously selected increases the complexity of the problem, but enables to consider alternatives that would be unexplored otherwise. In fact, the applications presented here produced unexpected results in terms of installed capacity and operating time.

The optimization problem was formulated under two alternative approaches: a mono-objective optimization with a single cost-based objective function, and a multi-objective optimization of capital cost and energy consumption. The main advantage of the second approach is that it produces a set of nondominated solutions. This is very useful when the capital cost and the operating cost are assumed by different agents. Additionally, there are some design criteria that are not explicitly included in the problem formulation, such as: redundancy, commonality of spare parts, maintenance strategy, and others. The approximate Pareto fronts obtained in the case studies provided a wide range of nondominated solutions that constitutes a starting point for a subsequent engineering analysis.

Modeling the performance functions is a critical point in formulating the optimal selection problem. This involves the necessity of including appropriate explanatory variables and establishing suitable functional forms. For instance, it can be seen in the chiller selection problem that, on average, including the outdoor temperature as an independent variable in both the capacity functions and the consumption functions increases the explanatory power in 3% and 23%, respectively. Additionally, these functions may be modeled as linear functions with a difference in explanatory power of only 1% on average. This linear approximation turned out to be very useful because problems that take hours or even days to be solved could be solved in a few seconds with a relative error of between 3% and 11%.

The results of the applications presented showed some counterintuitive facts. For

instance, the results in the chiller selection problem proved the benefits of having an installed capacity that exceeds by far the peak load. The chiller compressor performance is a function of the rotor rotation, but it also depends on certain geometrical features that may explain the unusual shapes of the COP curves at some points. It is also an unexpected result that some of the units selected for the FPSO platform are turned off most of the time. Another example revealing that the usual approach is not as reliable as it is thought to be is that the standard selection in the FPSO platforms is worse than all the nondominated solutions in terms of fuel consumption. The results are even more significant considering that the comparison is made with the standard selection at its optimal setting. This comparison was not made for the chiller plant because there is no standard selection for this application.

The NSGA-II, as well as other evolutionary algorithms, creates a random initial population. It may be interesting to explore alternative starting solutions based on prior knowledge. None of the cases studied in this work used an alternative initial guess. However, it might be an option worthy of consideration. Another important detail is the nature of the selection variable. In the first application this variable was treated as a nominal variable, but in the second application it was treated as a binary variable. Even though the optimization algorithm is not the core of this thesis, it is important to delve into these and other details that might improve the efficiency of the optimization process.

5.1 Future research

Applications. Besides the proven benefits in the contexts of chiller plants and FPSO platforms, the selection procedure may be applied in other engineering contexts as long as both the performance functions and the demand profiles are known. For instance, another potential application in the HVAC field is the selection of variable-speed pumps in hydronic cooling systems. This is a challenging problem because modeling the performance functions involves complex interrelated variables and parameters such as flow rate, head, efficiency and others.

Parameters. As well as depreciation rate and time value of money, additional important parameters might be considered in the analysis, such as equipment reliability and maintenance costs.

Optimization algorithms. Some problems have a complexity that makes it difficult to find optimal solutions. Many authors approach the optimal loading problem by using bio-inspired algorithms. There is an increasing number of algorithms to solve these optimization problems, and choosing the appropriate algorithm is an important issue. As a matter of fact, a wide range of scientific papers are devoted to comparing different al-

gorithms. The optimal selection problem also opens up a research field for benchmarking algorithms.

Bibliography

AHMADI, P.; DINCER, I. Thermodynamic analysis and thermoeconomic optimization of a dual pressure combined cycle power plant with a supplementary firing unit. *Energy Conversion and Management*, v. 52, n. 5, p. 2296–2308, 2011. ISSN 0196-8904.

AHMADI, P.; DINCER, I. Thermodynamic and exergoenvironmental analyses, and multi-objective optimization of a gas turbine power plant. *Applied Thermal Engineering*, v. 31, n. 14, p. 2529–2540, 2011. ISSN 1359-4311.

AHMADI, P.; DINCER, I.; ROSEN, M. A. Exergy, exergoeconomic and environmental analyses and evolutionary algorithm based multi-objective optimization of combined cycle power plants. *Energy*, v. 36, n. 10, p. 5886–5898, 2011. ISSN 0360-5442.

ALLAHYARZADEH-BIDGOLI, A. et al. Thermodynamic analysis and optimization of a multi-stage compression system for co2 injection unit: Nsga-ii and gradient-based methods. *Journal of the Brazilian Society of Mechanical Sciences and Engineering*, v. 43, p. 458, 2021. ISSN 1806-3691.

ANEEL. *Ranking das Tarifas*. 2021. ⟨https://www.aneel.gov.br/ranking-das-tarifas⟩. Online; accessed 22 June 2021.

ARAVELLI, A.; RAO, S. S. Energy optimization in chiller plants: A novel formulation and solution using a hybrid optimization technique. *Engineering Optimization*, Taylor and Francis, v. 45, n. 10, p. 1187–1203, 2013.

ARDAKANI, A. J.; ARDAKANI, F. F.; HOSSEINIAN, S. A novel approach for optimal chiller loading using particle swarm optimization. *Energy and Buildings*, v. 40, n. 12, p. 2177 – 2187, 2008. ISSN 0378-7788.

ASKARZADEH, A.; COELHO, L. dos S. Using two improved particle swarm optimization variants for optimization of daily electrical power consumption in multi-chiller systems. *Applied Thermal Engineering*, v. 89, p. 640 – 646, 2015. ISSN 1359-4311.

BARBOSA, Y. M. et al. Performance assessment of primary petroleum production cogeneration plants. *Energy*, v. 160, p. 233–244, 2018. ISSN 0360-5442.

BARRERA, J. J.; SAHLIT, A. (Ed.). *22nd International Congress of Mechanical Engineering - COBEM 2013*, v. 1674-1682 de *Exergy analysis and strategies for the waste heat recovery in offshore platforms*, (Exergy analysis and strategies for the waste heat recovery in offshore platforms, v. 1674-1682). Ribeirão Preto, SP, Brazil: [s.n.], 2013.

BENíTEZ-HIDALGO, A. et al. jmetalpy: A python framework for multi-objective optimization with metaheuristics. *Swarm and Evolutionary Computation*, v. 51, p. 100598, 2019. ISSN 2210-6502.

CAO, Y. et al. Thermodynamic analysis and optimization of a gas turbine and cascade co2 combined cycle. *Energy Conversion and Management*, v. 144, p. 193–204, 2017. ISSN 0196-8904.

Carranza Sánchez, Y. A.; de Oliveira, S. Exergy analysis of offshore primary petroleum processing plant with co2 capture. *Energy*, v. 88, p. 46–56, 2015. ISSN 0360-5442.

CHANG, Y.-C. A novel energy conservation method—optimal chiller loading. *Electric Power Systems Research*, v. 69, n. 2, p. 221 – 226, 2004. ISSN 0378-7796.

CHANG, Y.-C. Genetic algorithm based optimal chiller loading for energy conservation. *Applied Thermal Engineering*, v. 25, n. 17, p. 2800 – 2815, 2005. ISSN 1359-4311.

CHANG, Y.-C. An innovative approach for demand side management—optimal chiller loading by simulated annealing. *Energy*, v. 31, n. 12, p. 1883 – 1896, 2006. ISSN 0360-5442.

CHANG, Y.-C.; CHAN, T.-S.; LEE, W.-S. Economic dispatch of chiller plant by gradient method for saving energy. *Applied Energy*, v. 87, n. 4, p. 1096 – 1101, 2010. ISSN 0306-2619.

CHANG, Y.-C. et al. Evolution strategy based optimal chiller loading for saving energy. *Energy Conversion and Management*, v. 50, n. 1, p. 132 – 139, 2009. ISSN 0196-8904.

CHANG, Y.-C.; LIN, J.-K.; CHUANG, M.-H. Optimal chiller loading by genetic algorithm for reducing energy consumption. *Energy and Buildings*, v. 37, n. 2, p. 147 – 155, 2005. ISSN 0378-7788.

CHEN, D. et al. Optimal consumption modeling of multi–chiller system using a robust optimization algorithm with considering the measurement, control and threshold uncertainties. *Journal of Building Engineering*, v. 30, p. 101263, 2020. ISSN 2352-7102.

COELHO, L. dos S. et al. Optimal chiller loading for energy conservation using a new differential cuckoo search approach. *Energy*, v. 75, p. 237 – 243, 2014. ISSN 0360-5442.

COELHO, L. dos S.; MARIANI, V. C. Improved firefly algorithm approach applied to chiller loading for energy conservation. *Energy and Buildings*, v. 59, p. 273 – 278, 2013. ISSN 0378-7788.

CUCHIVAGUE, H. O. *Análise exergética de um sistema de injeção de CO2 para uma plataforma FPSO e sua integração com ciclo combinado e captura de carbono*. Tese (Doutorado) — Universidade Estadual de Campinas, Campinas, SP, 2015.

Czyzyk, J.; Mesnier, M. P.; Moré, J. J. The neos server. *IEEE Journal on Computational Science and Engineering*, v. 5, n. 3, p. 68, 1998.

da Silva, J. A.; de Oliveira Junior, S. Unit exergy cost and co2 emissions of offshore petroleum production. *Energy*, v. 147, p. 757–766, 2018. ISSN 0360-5442.

Damodaran, Aswath. *Costs of Capital by Industry (in USD)*. 2021. ⟨http://people.stern.nyu.edu/adamodar/New_Home_Page/dataarchived.html#discrate⟩. Online; accessed 20 December 2021.

DEB, K. *Multi-Objective Optimization Using Evolutionary Algorithms*. 1. ed. Wiley, 2009. Paperback. ISBN 0470743611. Disponível em: ⟨http://www.amazon.com/exec/obidos/redirect?tag=citeulike07-20&path=ASIN/0470743611⟩.

DEB, K. et al. A fast and elitist multiobjective genetic algorithm: Nsga-ii. *IEEE Transactions on Evolutionary Computation*, v. 6, n. 2, p. 182 – 197, 2002. ISSN 1941-0026.

Dolan, E. D. *The NEOS Server 4.0 Administrative Guide*. [S.l.], 2001.

DUAN, P.-y. et al. Solving chiller loading optimization problems using an improved teaching-learning-based optimization algorithm. *Optimal Control Applications and Methods*, v. 39, n. 1, p. 65–77, 2018.

FLóREZ-ORREGO, D. et al. Optimal design of power hubs for offshore petroleum platforms. *Energy*, v. 235, p. 121353, 2021. ISSN 0360-5442.

FLóREZ-ORREGO, D. et al. Centralized power generation with carbon capture on decommissioned offshore petroleum platforms. *Energy Conversion and Management*, v. 252, p. 115110, 2022. ISSN 0196-8904.

FOURER, R. *AMPL : a modeling language for mathematical programming*. 2. ed.. ed. San Francisco, Calif.: San Francisco, Calif. : Scientific Pr., 1996.

FUMERO, Y.; CORSANO, G.; MONTAGNA, J. M. A mixed integer linear programming model for simultaneous design and scheduling of flowshop plants. *Applied Mathematical Modelling*, v. 37, n. 4, p. 1652–1664, 2013. ISSN 0307-904X.

Gropp, W.; Moré, J. J. Optimization environments and the neos server. In: Buhman, M. D.; Iserles, A. (Ed.). *Approximation Theory and Optimization*. [S.l.]: Cambridge University Press, 1997. p. 167.

HIDALGO, J. I. et al. Analysis of multi-objective evolutionary algorithms to optimize dynamic data types in embedded systems. In: *Proceedings of the 10th Annual Conference on Genetic and Evolutionary Computation*. New York, NY, USA: Association for Computing Machinery, 2008. (GECCO '08), p. 1515–1522. ISBN 9781605581309.

JABARI, F.; MOHAMMADPOURFARD, M.; MOHAMMADI-IVATLOO, B. Energy efficient hourly scheduling of multi-chiller systems using imperialistic competitive algorithm. *Computers & Electrical Engineering*, v. 82, p. 106550, 2020. ISSN 0045-7906.

KHARE, V.; YAO, X.; DEB, K. Performance scaling of multi-objective evolutionary algorithms. In: FONSECA, C. M. et al. (Ed.). *Evolutionary Multi-Criterion Optimization*. Berlin, Heidelberg: Springer Berlin Heidelberg, 2003. p. 376–390. ISBN 978-3-540-36970-7.

KOCH, C.; CZIESLA, F.; TSATSARONIS, G. Optimization of combined cycle power plants using evolutionary algorithms. *Chemical Engineering and Processing: Process Intensification*, v. 46, n. 11, p. 1151–1159, 2007. ISSN 0255-2701. Special Issue on Process Optimization and Control in Chemical Engineering and Processing.

LEE, W.-S.; CHEN, Y.-T.; KAO, Y. Optimal chiller loading by differential evolution algorithm for reducing energy consumption. *Energy and Buildings*, v. 43, n. 2, p. 599 – 604, 2011. ISSN 0378-7788.

LEE, W.-S.; LIN, L.-C. Optimal chiller loading by particle swarm algorithm for reducing energy consumption. *Applied Thermal Engineering*, v. 29, n. 8, p. 1730 – 1734, 2009. ISSN 1359-4311.

LO, C.-C.; TSAI, S.-H.; LIN, B.-S. Economic dispatch of chiller plant by improved ripple bee swarm optimization algorithm for saving energy. *Applied Thermal Engineering*, v. 100, p. 1140 – 1148, 2016. ISSN 1359-4311.

MIN, S.; TANG, Z.; ROUYENDEGH, B. D. Inspired-based optimisation algorithm for solving energy-consuming reduction of chiller loading. *International Journal of Ambient Energy*, Taylor and Francis, v. 0, n. 0, p. 1–11, 2020.

MOHAGHEGHI, M.; SHAYEGAN, J. Thermodynamic optimization of design variables and heat exchangers layout in hrsgs for ccgt, using genetic algorithm. *Applied Thermal Engineering*, v. 29, n. 2, p. 290–299, 2009. ISSN 1359-4311.

MONSEF, H. et al. Comparison of evolutionary multi objective optimization algorithms in optimum design of water distribution network. *Ain Shams Engineering Journal*, v. 10, n. 1, p. 103 – 111, 2019. ISSN 2090-4479.

Nascimento Silva, F. C. et al. Comparative assessment of advanced power generation and carbon sequestration plants on offshore petroleum platforms. *Energy*, v. 203, p. 117737, 2020. ISSN 0360-5442.

Nascimento Silva, F. C.; FLóREZ-ORREGO, D.; de Oliveira Junior, S. Exergy assessment and energy integration of advanced gas turbine cycles on an offshore petroleum production platform. *Energy Conversion and Management*, v. 197, p. 111846, 2019. ISSN 0196-8904.

NGUYEN, T.-V. et al. Co2-mitigation options for the offshore oil and gas sector. *Applied Energy*, v. 161, p. 673–694, 2016. ISSN 0306-2619.

NJOKU, I. H. et al. Optimal thermal power plant selection for a tropical region using multi-criteria decision analysis. *Applied Thermal Engineering*, v. 179, p. 115706, 2020. ISSN 1359-4311.

NORD, L. O.; BOLLAND, O. Design and off-design simulations of combined cycles for offshore oil and gas installations. *Applied Thermal Engineering*, v. 54, n. 1, p. 85–91, 2013. ISSN 1359-4311.

PARGAS-CARMONA, L. A. et al. An optimization scheme for chiller selection in cooling plants. *Journal of Building Engineering*, v. 49, p. 104066, 2022. ISSN 2352-7102.

PARGAS-CARMONA, L. A. et al. Optimal selection of utility plants in oil and gas offshore platforms. *Journal of the Brazilian Society of Mechanical Sciences and Engineering*, v. 45, p. 248, 2023. ISSN 1806-3691.

PIEROBON, L. et al. Multi-objective optimization of organic rankine cycles for waste heat recovery: Application in an offshore platform. *Energy*, v. 58, p. 538–549, 2013. ISSN 0360-5442.

PRUITT, K. A. et al. A mixed-integer nonlinear program for the optimal design and dispatch of distributed generation systems. *Optimization and Engineering*, v. 15, n. 1, p. 167–197, 2014. ISSN 1573-2924.

REIS, M. M. L.; GUILLEN, J. A. V.; GALLO, W. L. Off-design performance analysis and optimization of the power production by an organic rankine cycle coupled with a gas turbine in an offshore oil platform. *Energy Conversion and Management*, v. 196, p. 1037–1050, 2019. ISSN 0196-8904.

REIS, M. M. L. dos; GALLO, W. L. R. Study of waste heat recovery potential and optimization of the power production by an organic rankine cycle in an fpso unit. *Energy Conversion and Management*, v. 157, p. 409–422, 2018.

REZAIE, A.; TSATSARONIS, G.; HELLWIG, U. Thermal design and optimization of a heat recovery steam generator in a combined-cycle power plant by applying a genetic algorithm. *Energy*, v. 168, p. 346–357, 2019. ISSN 0360-5442.

Riboldi, L.; Nord, L. O. Lifetime assessment of combined cycles for cogeneration of power and heat in offshore oil and gas installations. *Energies*, v. 10, p. 111846, 2017.

ROVIRA, A. et al. Thermoeconomic optimisation of heat recovery steam generators of combined cycle gas turbine power plants considering off-design operation. *Energy Conversion and Management*, v. 52, n. 4, p. 1840–1849, 2011. ISSN 0196-8904.

SAHINIDIS, N. V. *BARON 21.1.13: Global Optimization of Mixed-Integer Nonlinear Programs,* User's Manual. [S.l.], 2017.

SAYYAADI, H.; MEHRABIPOUR, R. Efficiency enhancement of a gas turbine cycle using an optimized tubular recuperative heat exchanger. *Energy*, v. 38, n. 1, p. 362–375, 2012. ISSN 0360-5442.

SAYYAD, A. S.; AMMAR, H. Pareto-optimal search-based software engineering (posbse): A literature survey. In: *2013 2nd International Workshop on Realizing Artificial Intelligence Synergies in Software Engineering (RAISE)*. [S.l.: s.n.], 2013. p. 21–27.

SHAMOUSHAKI FARROKH GHANATIR, M. E. M.; AHMADI, A. Exergy and exergoeconomic analysis and multi-objective optimisation of gas turbine power plant by evolutionary algorithms. case study: Aliabad katoul power plant. *International Journal of Exergy*, v. 22, n. 3, p. 279–307, 2017. ISSN 1742-8297.

SOHRABI, F. et al. Optimal chiller loading for saving energy by exchange market algorithm. *Energy and Buildings*, v. 169, p. 245 – 253, 2018. ISSN 0378-7788.

STANFORD, H. *Effective Building Maintenance - Protection of Capital Assets*. Lilburn, GA: The Fairmont Press Inc., 2010.

SULAIMAN, M. H. et al. A new swarm intelligence approach for optimal chiller loading for energy conservation. *Procedia - Social and Behavioral Sciences*, v. 129, p. 483 – 488, 2014. ISSN 1877-0428. 2nd International Conference on Innovation, Management and Technology Research.

TAWARMALANI, M.; SAHINIDIS, N. V. A polyhedral branch-and-cut approach to global optimization. *Mathematical Programming*, v. 103, p. 225–249, 2005.

TEIMOURZADEH, H.; JABARI, F.; MOHAMMADI-IVATLOO, B. An augmented group search optimization algorithm for optimal cooling-load dispatch in multi-chiller plants. *Computers & Electrical Engineering*, v. 85, p. 106434, 2020. ISSN 0045-7906.

THANGAVELU, S. R.; MYAT, A.; KHAMBADKONE, A. Energy optimization methodology of multi-chiller plant in commercial buildings. *Energy*, v. 123, p. 64 – 76, 2017. ISSN 0360-5442.

THERMOFLOW Inc. *THERMOFLEX*. 2021. Jacksonville FL 32246, USA.

TIAN, C. et al. A method for cop prediction of an on-site screw chiller applied in cinema. *International Journal of Refrigeration*, v. 98, p. 459–467, 2019. ISSN 0140-7007.

TIAN, E. et al. Application of new optimisation model for multi-chiller system consumption. *International Journal of Ambient Energy*, Taylor and Francis, v. 0, n. 0, p. 1–13, 2019.

U.S. Energy Information Administration (EIA). *Henry Hub Natural Gas Spot Price (Dollars per Million Btu)*. 2021. ⟨https://www.eia.gov/dnav/ng/hist/rngwhhda.htm⟩. Online; accessed 20 December 2021.

VELOSO, T. *Otimização da Implantação de Sistemas ORC em uma FPSO Brasileira*. Tese (Doutorado) — Universidade Federal de Itajubá, Itajubá, 2015.

WANG, L. et al. Superstructure-free synthesis and optimization of thermal power plants. *Energy*, v. 91, p. 700–711, 2015. ISSN 0360-5442.

WENHAN, X. et al. Improved grasshopper optimization algorithm to solve energy consuming reduction of chiller loading. *Energy Sources, Part A: Recovery, Utilization, and Environmental Effects*, Taylor and Francis, v. 0, n. 0, p. 1–14, 2019.

WILDING, P. R.; MURRAY, N. R.; MEMMOTT, M. J. The use of multi-objective optimization to improve the design process of nuclear power plant systems. *Annals of Nuclear Energy*, v. 137, p. 107079, 2020. ISSN 0306-4549.

YU, F.; CHAN, K. An alternative approach for the performance rating of air-cooled chillers used in air-conditioned buildings. *Building and Environment*, v. 41, n. 12, p. 1723–1730, 2006. ISSN 0360-1323.

YU, J. et al. Optimal chiller loading in hvac system using a novel algorithm based on the distributed framework. *Journal of Building Engineering*, v. 28, p. 101044, 2020. ISSN 2352-7102.

ZHENG, Z. xin; LI, J. qing. Optimal chiller loading by improved invasive weed optimization algorithm for reducing energy consumption. *Energy and Buildings*, v. 161, p. 80 – 88, 2018. ISSN 0378-7788.

ZHENG, Z. xin; LI, J. qing; DUAN, P. yong. Optimal chiller loading by improved artificial fish swarm algorithm for energy saving. *Mathematics and Computers in Simulation*, v. 155, p. 227 – 243, 2019. ISSN 0378-4754. International Conference on Mathematical Modeling and Computational Methods in Science and Engineering.

Appendix A

Chillers performance data

Table A.1: Performance data - Model 140

Nom. cap. (TR)	Outdoor temp. (°F)	Load ratio	Capacity (TR)	Power (kW)
140	115	1.00	131.9	197.2
140	115	0.90	118.7	171.4
140	115	0.80	105.5	151.3
140	115	0.70	92.35	129
140	115	0.60	79.16	108.6
140	115	0.50	65.96	90.33
140	115	0.40	52.77	73.4
140	115	0.30	39.58	55.01
140	115	0.20	26.39	36.98
140	115	0.13	16.49	24.05
140	95	1.00	143.8	157.4
140	95	0.90	129.4	136.3
140	95	0.80	115	116.7
140	95	0.70	100.7	98.94
140	95	0.60	86.27	82.23
140	95	0.50	71.89	67.66
140	95	0.40	57.52	54.21
140	95	0.30	43.14	41.79
140	95	0.20	28.76	27.38
140	95	0.13	17.97	17.54
140	80	1.00	150.3	131.1
140	80	0.90	135.2	113.5
140	80	0.80	120.2	96.98
140	80	0.70	105.2	81.88
140	80	0.60	90.16	68.4
140	80	0.50	75.13	55.21
140	80	0.40	60.11	44.4
140	80	0.30	45.08	34.88
140	80	0.20	30.05	22.58
140	80	0.13	18.78	14.05
140	65	1.00	155.6	109.1
140	65	0.90	140	92.96
140	65	0.80	124.5	78.39
140	65	0.70	108.9	65.6
140	65	0.60	93.36	53.58
140	65	0.50	77.8	43.1
140	65	0.40	62.24	33.28
140	65	0.30	46.68	27.32
140	65	0.20	31.12	16.93
140	65	0.13	19.45	10.35
140	55	1.00	157.9	94.49
140	55	0.90	142.1	80.18
140	55	0.80	126.3	67.54
140	55	0.70	110.5	55.96
140	55	0.60	94.75	44.77
140	55	0.50	78.96	35.38
140	55	0.40	63.17	27.27
140	55	0.30	47.38	22.96
140	55	0.20	31.58	13.88
140	55	0.13	19.74	8.585

Table A.2: Performance data - Model 160

Nom. cap. (TR)	Outdoor temp. (°F)	Load ratio	Capacity (TR)	Power (kW)
160	115	1.00	150.5	219.9
160	115	0.90	135.4	192
160	115	0.80	120.4	165.7
160	115	0.70	105.3	141.6
160	115	0.60	90.29	118.9
160	115	0.50	75.24	98.46
160	115	0.40	60.19	79.47
160	115	0.30	45.14	61.8
160	115	0.20	30.1	40.05
160	115	0.13	18.81	26.44
160	95	1.00	162.7	175
160	95	0.90	146.4	150.4
160	95	0.80	130.2	128.7
160	95	0.70	113.9	108.8
160	95	0.60	97.62	90.63
160	95	0.50	81.35	74.26
160	95	0.40	65.08	59.13
160	95	0.30	48.81	45.51
160	95	0.20	32.54	29.86
160	95	0.13	20.34	19.29
160	80	1.00	170.4	146.9
160	80	0.90	153.4	127
160	80	0.80	136.3	108.5
160	80	0.70	119.3	90.9
160	80	0.60	102.3	74.9
160	80	0.50	85.22	61.1
160	80	0.40	68.17	47.27
160	80	0.30	51.13	36.14
160	80	0.20	34.09	23.88
160	80	0.13	21.3	15.19
160	65	1.00	175.5	122.9
160	65	0.90	158	103.8
160	65	0.80	140.4	87.35
160	65	0.70	122.9	72.66
160	65	0.60	105.3	59.55
160	65	0.50	87.77	47.65
160	65	0.40	70.21	36.84
160	65	0.30	52.66	26.96
160	65	0.20	35.11	18.72
160	65	0.13	21.94	11.36
160	55	1.00	178.8	107
160	55	0.90	160.9	90.43
160	55	0.80	143	75.82
160	55	0.70	125.1	62.77
160	55	0.60	107.3	50.58
160	55	0.50	89.39	39.75
160	55	0.40	71.51	30.49
160	55	0.30	53.63	23.03
160	55	0.20	35.75	15.42
160	55	0.13	22.35	9.652

Table A.3: Performance data - Model 180

Nom. cap. (TR)	Outdoor temp. (°F)	Load ratio	Capacity (TR)	Power (kW)
180	115	1.00	166.2	249.7
180	115	0.90	149.6	215.5
180	115	0.80	133	184.7
180	115	0.70	116.3	156.5
180	115	0.60	99.73	130.9
180	115	0.50	83.11	107.6
180	115	0.40	66.48	86.08
180	115	0.30	49.86	66.31
180	115	0.20	33.24	43.38
180	115	0.13	20.78	28.7
180	95	1.00	180.7	201.2
180	95	0.90	162.7	171.5
180	95	0.80	144.6	145.3
180	95	0.70	126.5	122
180	95	0.60	108.4	101.1
180	95	0.50	90.37	82.05
180	95	0.40	72.29	64.85
180	95	0.30	54.22	49.27
180	95	0.20	36.15	32.74
180	95	0.13	22.59	21.15
180	80	1.00	188.6	170.1
180	80	0.90	169.7	143.5
180	80	0.80	150.9	122
180	80	0.70	132	102.3
180	80	0.60	113.2	83.58
180	80	0.50	94.3	67.65
180	80	0.40	75.44	52.17
180	80	0.30	56.58	39.66
180	80	0.20	37.72	26.44
180	80	0.13	23.58	16.58
180	65	1.00	195.4	143.4
180	65	0.90	175.8	120.6
180	65	0.80	156.3	100.2
180	65	0.70	136.7	82.71
180	65	0.60	117.2	67.23
180	65	0.50	97.68	53.43
180	65	0.40	78.14	41.1
180	65	0.30	58.61	29.7
180	65	0.20	39.07	20.83
180	65	0.13	24.42	12.46
180	55	1.00	198.7	126.5
180	55	0.90	178.8	104.9
180	55	0.80	158.9	87.1
180	55	0.70	139.1	71.51
180	55	0.60	119.2	57.76
180	55	0.50	99.33	44.77
180	55	0.40	79.46	33.92
180	55	0.30	59.6	25.68
180	55	0.20	39.73	17.25
180	55	0.13	24.83	10.57

Table A.4: Performance data - Model 200

Nom. cap. (TR)	Outdoor temp. (°F)	Load ratio	Capacity (TR)	Power (kW)
200	115	1.00	183.5	276.9
200	115	0.90	165.1	236.9
200	115	0.80	146.8	200.7
200	115	0.70	128.4	169.2
200	115	0.60	110.1	140.1
200	115	0.50	91.74	115
200	115	0.40	73.39	92.14
200	115	0.30	55.05	70.93
200	115	0.20	36.7	46.46
200	115	0.13	22.94	30.53
200	95	1.00	198.5	222.2
200	95	0.90	178.6	187.9
200	95	0.80	158.8	158.6
200	95	0.70	138.9	132.2
200	95	0.60	119.1	108.6
200	95	0.50	99.23	88.11
200	95	0.40	79.38	69.64
200	95	0.30	59.54	52.95
200	95	0.20	39.69	35.17
200	95	0.13	24.81	22.68
200	80	1.00	207.6	189.5
200	80	0.90	186.8	160.5
200	80	0.80	166.1	134.3
200	80	0.70	145.3	112.2
200	80	0.60	124.5	90.55
200	80	0.50	103.8	72.33
200	80	0.40	83.03	56.43
200	80	0.30	62.27	42.38
200	80	0.20	41.52	28.58
200	80	0.13	25.95	18.06
200	65	1.00	214.2	160.5
200	65	0.90	192.8	133.3
200	65	0.80	171.4	110.6
200	65	0.70	150	90.64
200	65	0.60	128.5	73.22
200	65	0.50	107.1	57.69
200	65	0.40	85.69	44.4
200	65	0.30	64.26	32.34
200	65	0.20	42.84	22.48
200	65	0.13	26.78	13.59
200	55	1.00	219	141.7
200	55	0.90	197.1	117.8
200	55	0.80	175.2	97.1
200	55	0.70	153.3	79.29
200	55	0.60	131.4	63.5
200	55	0.50	109.5	49.21
200	55	0.40	87.59	36.86
200	55	0.30	65.69	27.09
200	55	0.20	43.79	18.75
200	55	0.13	27.37	11.81

Table A.5: Performance data - Model 225

Nom. cap. (TR)	Outdoor temp. (°F)	Load ratio	Capacity (TR)	Power (kW)
225	115	1.00	199.8	309.6
225	115	0.90	179.8	270.7
225	115	0.80	159.9	233.9
225	115	0.70	139.9	199.3
225	115	0.60	119.9	167.7
225	115	0.50	99.92	139.9
225	115	0.40	79.93	113.6
225	115	0.30	59.95	88.03
225	115	0.20	39.97	59.99
225	115	0.13	24.98	38.65
225	95	1.00	219.4	247.6
225	95	0.90	197.5	213.9
225	95	0.80	175.5	182.8
225	95	0.70	153.6	153.2
225	95	0.60	131.6	126.5
225	95	0.50	109.7	102.4
225	95	0.40	87.76	81.21
225	95	0.30	65.82	61.48
225	95	0.20	43.88	40.89
225	95	0.13	27.42	25.24
225	80	1.00	231.3	206.5
225	80	0.90	208.2	178
225	80	0.80	185.1	152.5
225	80	0.70	161.9	127.2
225	80	0.60	138.8	105
225	80	0.50	115.7	84.79
225	80	0.40	92.53	66.43
225	80	0.30	69.4	50.78
225	80	0.20	46.27	34.04
225	80	0.13	28.92	21.69
225	65	1.00	240.1	176
225	65	0.90	216.1	150
225	65	0.80	192.1	126.2
225	65	0.70	168.1	104.1
225	65	0.60	144.1	84.24
225	65	0.50	120	66.53
225	65	0.40	96.04	51.59
225	65	0.30	72.03	38.25
225	65	0.20	48.02	25.92
225	65	0.13	30.01	15.55
225	55	1.00	245.5	154.7
225	55	0.90	220.9	131.3
225	55	0.80	196.4	110.2
225	55	0.70	171.8	90.59
225	55	0.60	147.3	72.68
225	55	0.50	122.7	56.14
225	55	0.40	98.2	43.23
225	55	0.30	73.65	32.29
225	55	0.20	49.1	21.84
225	55	0.13	30.69	13.45

Table A.6: Performance data - Model 250

Nom. cap. (TR)	Outdoor temp. (°F)	Load ratio	Capacity (TR)	Power (kW)
250	115	1.00	235.3	362.6
250	115	0.90	211.8	321.9
250	115	0.80	188.2	282
250	115	0.70	164.7	245.7
250	115	0.60	141.2	211.2
250	115	0.50	117.6	175.6
250	115	0.40	94.11	142.2
250	115	0.30	70.58	111.2
250	115	0.20	47.06	71.76
250	115	0.13	29.41	47.08
250	95	1.00	260	288.2
250	95	0.90	234	252
250	95	0.80	208	218.1
250	95	0.70	182	185.2
250	95	0.60	156	154.4
250	95	0.50	130	125.5
250	95	0.40	104	98.74
250	95	0.30	78.01	73.86
250	95	0.20	52.01	49.93
250	95	0.13	32.5	30.44
250	80	1.00	274.7	238.5
250	80	0.90	247.2	208.5
250	80	0.80	219.7	180.2
250	80	0.70	192.3	151.8
250	80	0.60	164.8	126.4
250	80	0.50	137.3	102.5
250	80	0.40	109.9	80.81
250	80	0.30	82.4	61.22
250	80	0.20	54.94	40.9
250	80	0.13	34.33	26.07
250	65	1.00	285.4	203.9
250	65	0.90	256.9	176.5
250	65	0.80	228.3	149.6
250	65	0.70	199.8	125.6
250	65	0.60	171.3	102
250	65	0.50	142.7	81.08
250	65	0.40	114.2	62.98
250	65	0.30	85.63	46.86
250	65	0.20	57.09	31.9
250	65	0.13	35.68	19.32
250	55	1.00	292.6	180.4
250	55	0.90	263.3	154.7
250	55	0.80	234	131.5
250	55	0.70	204.8	108.6
250	55	0.60	175.5	87.79
250	55	0.50	146.3	68.54
250	55	0.40	117	53.19
250	55	0.30	87.77	39.31
250	55	0.20	58.51	27.03
250	55	0.13	36.57	16.15

Table A.7: Performance data - Model 275

Nom. cap. (TR)	Outdoor temp. (°F)	Load ratio	Capacity (TR)	Power (kW)
275	115	1.00	250.1	390.9
275	115	0.90	225.1	344.1
275	115	0.80	200.1	301.6
275	115	0.70	175.1	260.7
275	115	0.60	150.1	223.6
275	115	0.50	125	186.5
275	115	0.40	100	150.3
275	115	0.30	75.03	116.8
275	115	0.20	50.02	75.82
275	115	0.13	31.26	49.84
275	95	1.00	275.7	310.2
275	95	0.90	248.1	271.3
275	95	0.80	220.5	233.6
275	95	0.70	193	198.9
275	95	0.60	165.4	164.9
275	95	0.50	137.8	134
275	95	0.40	110.3	104.9
275	95	0.30	82.7	78.55
275	95	0.20	55.13	52.99
275	95	0.13	34.46	32.47
275	80	1.00	291.8	260.2
275	80	0.90	262.6	224.5
275	80	0.80	233.4	194.2
275	80	0.70	204.2	163.1
275	80	0.60	175.1	136
275	80	0.50	145.9	109.4
275	80	0.40	116.7	85.59
275	80	0.30	87.53	64.79
275	80	0.20	58.35	43.3
275	80	0.13	36.47	27.54
275	65	1.00	302.4	220.9
275	65	0.90	272.1	190.3
275	65	0.80	241.9	161.7
275	65	0.70	211.7	135.2
275	65	0.60	181.4	109.7
275	65	0.50	151.2	86.98
275	65	0.40	120.9	66.94
275	65	0.30	90.71	49.65
275	65	0.20	60.47	33.89
275	65	0.13	37.8	20.59
275	55	1.00	310.1	195.8
275	55	0.90	279.1	168.5
275	55	0.80	248.1	141.9
275	55	0.70	217.1	117.8
275	55	0.60	186	94.6
275	55	0.50	155	74.01
275	55	0.40	124	56.69
275	55	0.30	93.02	41.86
275	55	0.20	62.01	28.79
275	55	0.13	38.76	17.25

Table A.8: Performance data - Model 300

Nom. cap. (TR)	Outdoor temp. (°F)	Load ratio	Capacity (TR)	Power (kW)
300	115	1.00	263	400.3
300	115	0.90	236.7	350.9
300	115	0.80	210.4	307
300	115	0.70	184.1	264.1
300	115	0.60	157.8	223.2
300	115	0.50	131.5	183.7
300	115	0.40	105.2	147.4
300	115	0.30	78.91	112.7
300	115	0.20	52.61	74.36
300	115	0.13	32.88	48.24
300	95	1.00	289.3	322.6
300	95	0.90	260.4	276.5
300	95	0.80	231.4	236.8
300	95	0.70	202.5	199.9
300	95	0.60	173.6	166.4
300	95	0.50	144.7	133.9
300	95	0.40	115.7	104.7
300	95	0.30	86.79	77.94
300	95	0.20	57.86	52.93
300	95	0.13	36.16	32.68
300	80	1.00	304.5	270.1
300	80	0.90	274.1	231.4
300	80	0.80	243.6	197.5
300	80	0.70	213.2	166.9
300	80	0.60	182.7	137.5
300	80	0.50	152.3	110.7
300	80	0.40	121.8	85.54
300	80	0.30	91.36	64.55
300	80	0.20	60.91	43.39
300	80	0.13	38.07	27.21
300	65	1.00	315.6	231.4
300	65	0.90	284	196
300	65	0.80	252.4	164.6
300	65	0.70	220.9	136.7
300	65	0.60	189.3	111.3
300	65	0.50	157.8	87.65
300	65	0.40	126.2	67.08
300	65	0.30	94.67	49.48
300	65	0.20	63.11	34.03
300	65	0.13	39.44	20.77
300	55	1.00	323.4	206.2
300	55	0.90	291.1	173.9
300	55	0.80	258.7	146.4
300	55	0.70	226.4	119.6
300	55	0.60	194.1	96.34
300	55	0.50	161.7	75.24
300	55	0.40	129.4	56.77
300	55	0.30	97.03	41.97
300	55	0.20	64.69	28.85
300	55	0.13	40.43	17.55

Table A.9: Performance data - Model 325

Nom. cap. (TR)	Outdoor temp. (°F)	Load ratio	Capacity (TR)	Power (kW)
325	115	1.00	287.3	433.9
325	115	0.90	258.5	384.8
325	115	0.80	229.8	336
325	115	0.70	201.1	280.6
325	115	0.60	172.4	228.7
325	115	0.50	143.6	187.8
325	115	0.40	114.9	151.4
325	115	0.30	86.18	117.5
325	115	0.20	57.45	76.42
325	115	0.13	35.91	50.17
325	95	1.00	315.1	351.6
325	95	0.90	283.6	312.6
325	95	0.80	252.1	264.6
325	95	0.70	220.6	216.2
325	95	0.60	189.1	174.8
325	95	0.50	157.6	139.3
325	95	0.40	126	109.6
325	95	0.30	94.53	82.3
325	95	0.20	63.02	55.39
325	95	0.13	39.39	34.99
325	80	1.00	329.3	303.2
325	80	0.90	296.4	259
325	80	0.80	263.4	219
325	80	0.70	230.5	182.6
325	80	0.60	197.6	145.2
325	80	0.50	164.7	115.2
325	80	0.40	131.7	88.7
325	80	0.30	98.79	67.67
325	80	0.20	65.86	44.98
325	80	0.13	41.16	28.57
325	65	1.00	340.6	259.5
325	65	0.90	306.6	219.3
325	65	0.80	272.5	183.2
325	65	0.70	238.5	149.1
325	65	0.60	204.4	118.2
325	65	0.50	170.3	91.02
325	65	0.40	136.3	69.52
325	65	0.30	102.2	51.19
325	65	0.20	68.13	35.26
325	65	0.13	42.58	21.64
325	55	1.00	348.5	229.9
325	55	0.90	313.6	193.6
325	55	0.80	278.8	161.9
325	55	0.70	243.9	131
325	55	0.60	209.1	102.3
325	55	0.50	174.2	77.58
325	55	0.40	139.4	58.46
325	55	0.30	104.5	44.46
325	55	0.20	69.69	29.69
325	55	0.13	43.56	18.75

Table A.10: Performance data - Model 350

Nom. cap. (TR)	Outdoor temp. (°F)	Load ratio	Capacity (TR)	Power (kW)
350	115	1.00	319.8	486.2
350	115	0.90	287.8	421.8
350	115	0.80	255.9	369
350	115	0.70	223.9	315.5
350	115	0.60	191.9	265.1
350	115	0.50	159.9	218.2
350	115	0.40	127.9	174.7
350	115	0.30	95.94	132.4
350	115	0.20	63.96	92.68
350	115	0.13	39.98	60.95
350	95	1.00	350.6	394.9
350	95	0.90	315.5	339.6
350	95	0.80	280.5	289.9
350	95	0.70	245.4	244.1
350	95	0.60	210.3	202
350	95	0.50	175.3	163.6
350	95	0.40	140.2	127.6
350	95	0.30	105.2	94.09
350	95	0.20	70.11	66.75
350	95	0.13	43.82	41.32
350	80	1.00	369.6	335.7
350	80	0.90	332.7	286.7
350	80	0.80	295.7	243.9
350	80	0.70	258.7	204.5
350	80	0.60	221.8	169.1
350	80	0.50	184.8	135.3
350	80	0.40	147.8	104.6
350	80	0.30	110.9	76.67
350	80	0.20	73.92	55.25
350	80	0.13	46.2	34.43
350	65	1.00	384.9	288.6
350	65	0.90	346.4	243.4
350	65	0.80	307.9	203.9
350	65	0.70	269.5	167.9
350	65	0.60	231	135.2
350	65	0.50	192.5	106.7
350	65	0.40	154	81.04
350	65	0.30	115.5	58.12
350	65	0.20	76.99	44.09
350	65	0.13	48.12	26.53
350	55	1.00	394.8	255.4
350	55	0.90	355.4	214.7
350	55	0.80	315.9	178.8
350	55	0.70	276.4	145.4
350	55	0.60	236.9	116.9
350	55	0.50	197.4	91.95
350	55	0.40	157.9	69.7
350	55	0.30	118.5	50.38
350	55	0.20	78.97	37.8
350	55	0.13	49.36	22.34

Table A.11: Performance data - Model 400

Nom. cap. (TR)	Outdoor temp. (°F)	Load ratio	Capacity (TR)	Power (kW)
400	115	1.00	369.6	552.4
400	115	0.90	332.7	478
400	115	0.80	295.7	421.2
400	115	0.70	258.7	362.3
400	115	0.60	221.8	308.6
400	115	0.50	184.8	255.8
400	115	0.40	147.9	205.9
400	115	0.30	110.9	156.4
400	115	0.20	73.93	103.9
400	115	0.13	46.2	64.81
400	95	1.00	403.9	456.5
400	95	0.90	363.5	392.8
400	95	0.80	323.1	334.1
400	95	0.70	282.7	284.4
400	95	0.60	242.3	237
400	95	0.50	202	193.3
400	95	0.40	161.6	151.8
400	95	0.30	121.2	120.1
400	95	0.20	80.78	76.65
400	95	0.13	50.49	46.52
400	80	1.00	426.8	391.1
400	80	0.90	384.1	333.7
400	80	0.80	341.4	282.9
400	80	0.70	298.7	237.6
400	80	0.60	256.1	197.9
400	80	0.50	213.4	159.6
400	80	0.40	170.7	125.4
400	80	0.30	128	100.4
400	80	0.20	85.35	63.33
400	80	0.13	53.35	38.3
400	65	1.00	445.4	337.5
400	65	0.90	400.9	282.6
400	65	0.80	356.3	235.3
400	65	0.70	311.8	193.5
400	65	0.60	267.3	156.9
400	65	0.50	222.7	124.4
400	65	0.40	178.2	93.77
400	65	0.30	133.6	79.89
400	65	0.20	89.09	47.6
400	65	0.13	55.68	27.53
400	55	1.00	457.1	296
400	55	0.90	411.4	247.7
400	55	0.80	365.7	204.8
400	55	0.70	320	167.7
400	55	0.60	274.3	135.9
400	55	0.50	228.6	107.5
400	55	0.40	182.9	81.18
400	55	0.30	137.1	69.29
400	55	0.20	91.43	41.24
400	55	0.13	57.14	23.95

Table A.12: Performance data - Model 450

Nom. cap. (TR)	Outdoor temp. (°F)	Load ratio	Capacity (TR)	Power (kW)
450	115	1.00	416.8	615.9
450	115	0.90	375.1	537.1
450	115	0.80	333.4	461.6
450	115	0.70	291.7	394.4
450	115	0.60	250.1	334.9
450	115	0.50	208.4	277.6
450	115	0.40	166.7	224
450	115	0.30	125	170.6
450	115	0.20	83.35	112.9
450	115	0.13	52.09	71.64
450	95	1.00	454.6	514.2
450	95	0.90	409.1	438
450	95	0.80	363.7	369.8
450	95	0.70	318.2	311.7
450	95	0.60	272.8	260
450	95	0.50	227.3	211.6
450	95	0.40	181.8	167.1
450	95	0.30	136.4	122.4
450	95	0.20	90.92	84.36
450	95	0.13	56.82	51.25
450	80	1.00	480.4	444.1
450	80	0.90	432.3	375.3
450	80	0.80	384.3	315.6
450	80	0.70	336.3	262.9
450	80	0.60	288.2	218
450	80	0.50	240.2	176.3
450	80	0.40	192.1	137.4
450	80	0.30	144.1	101
450	80	0.20	96.07	69.34
450	80	0.13	60.05	42.23
450	65	1.00	502	385.5
450	65	0.90	451.8	323.1
450	65	0.80	401.6	266.3
450	65	0.70	351.4	217.5
450	65	0.60	301.2	175.5
450	65	0.50	251	138.8
450	65	0.40	200.8	105.4
450	65	0.30	150.6	72.41
450	65	0.20	100.4	53.41
450	65	0.13	62.76	30.36
450	55	1.00	514.8	343.3
450	55	0.90	463.3	284
450	55	0.80	411.8	233.1
450	55	0.70	360.3	189.4
450	55	0.60	308.9	152.4
450	55	0.50	257.4	119.9
450	55	0.40	205.9	91.07
450	55	0.30	154.4	63.1
450	55	0.20	103	46.14
450	55	0.13	64.34	26.21

Table A.13: Performance data - Model 500

Nom. cap. (TR)	Outdoor temp. (°F)	Load ratio	Capacity (TR)	Power (kW)
500	115	1.00	459.8	691.7
500	115	0.90	413.8	599.6
500	115	0.80	367.8	510.4
500	115	0.70	321.9	428.8
500	115	0.60	275.9	356.3
500	115	0.50	229.9	291.5
500	115	0.40	183.9	231.9
500	115	0.30	137.9	175.4
500	115	0.20	91.96	116.8
500	115	0.13	57.47	73.27
500	95	1.00	501.9	577.8
500	95	0.90	451.7	495.1
500	95	0.80	401.5	415.5
500	95	0.70	351.3	345.4
500	95	0.60	301.1	282.5
500	95	0.50	250.9	226.4
500	95	0.40	200.8	176.4
500	95	0.30	150.6	129.6
500	95	0.20	100.4	88.91
500	95	0.13	62.74	53.38
500	80	1.00	528.9	497.7
500	80	0.90	476	426.6
500	80	0.80	423.1	356.2
500	80	0.70	370.2	293.2
500	80	0.60	317.4	239.1
500	80	0.50	264.5	190.5
500	80	0.40	211.6	145.1
500	80	0.30	158.7	105.9
500	80	0.20	105.8	73.42
500	80	0.13	66.12	43.18
500	65	1.00	552.5	437.4
500	65	0.90	497.3	369
500	65	0.80	442	304.5
500	65	0.70	386.8	246.9
500	65	0.60	331.5	196.3
500	65	0.50	276.3	152.4
500	65	0.40	221	114.4
500	65	0.30	165.8	78.55
500	65	0.20	110.5	57.85
500	65	0.13	69.07	31.53
500	55	1.00	567.5	389.4
500	55	0.90	510.7	329.3
500	55	0.80	454	269.2
500	55	0.70	397.2	217.1
500	55	0.60	340.5	171.4
500	55	0.50	283.7	132.4
500	55	0.40	227	99.42
500	55	0.30	170.2	68.65
500	55	0.20	113.5	50.31
500	55	0.13	70.94	27.5

Appendix B

Chillers performance curves

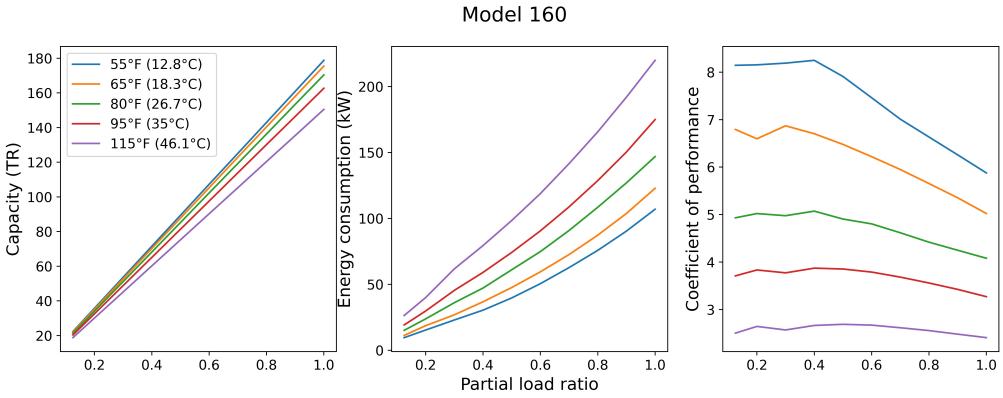

Figure B.1: Performance curves - Model 160

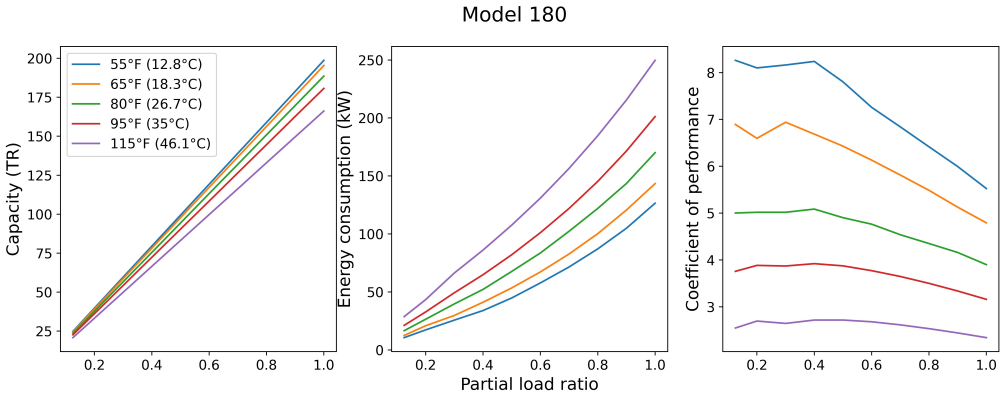

Figure B.2: Performance curves - Model 180

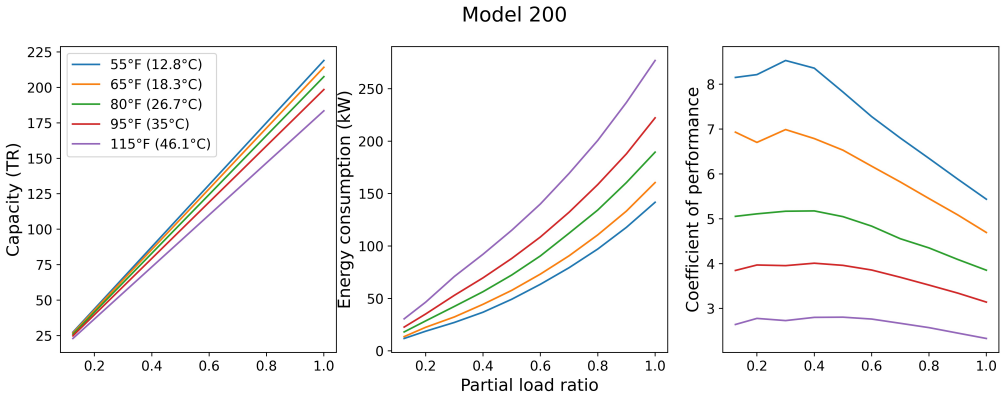

Figure B.3: Performance curves - Model 200

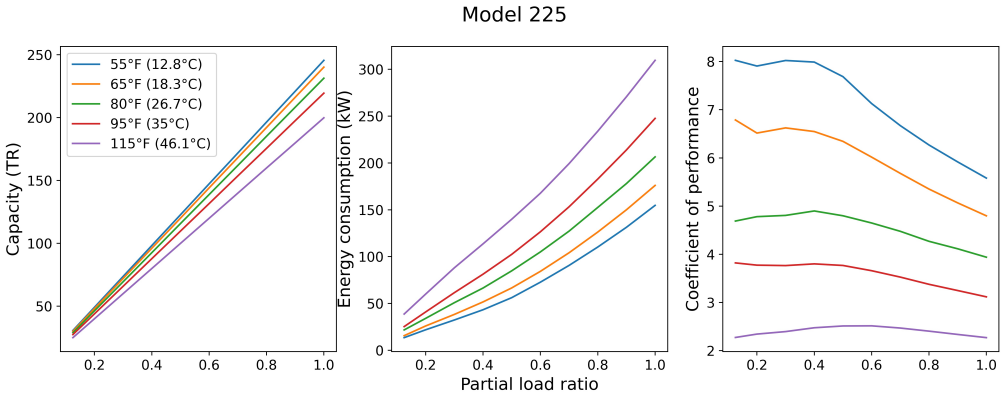

Figure B.4: Performance curves - Model 225

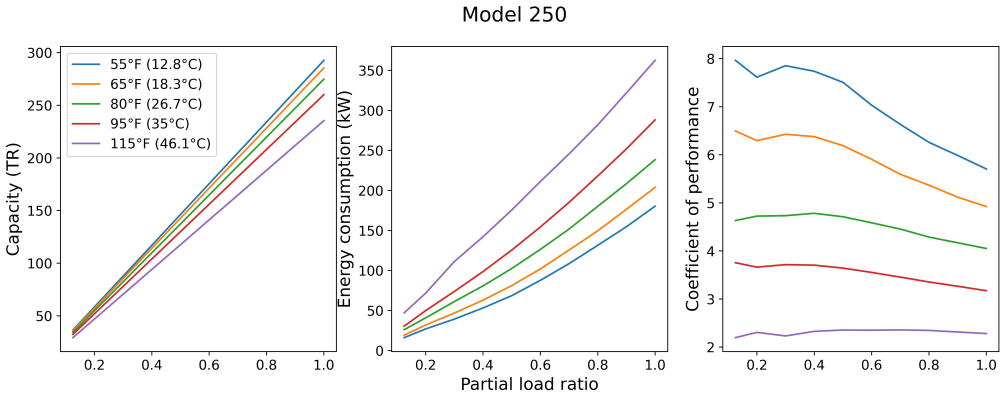

Figure B.5: Performance curves - Model 250

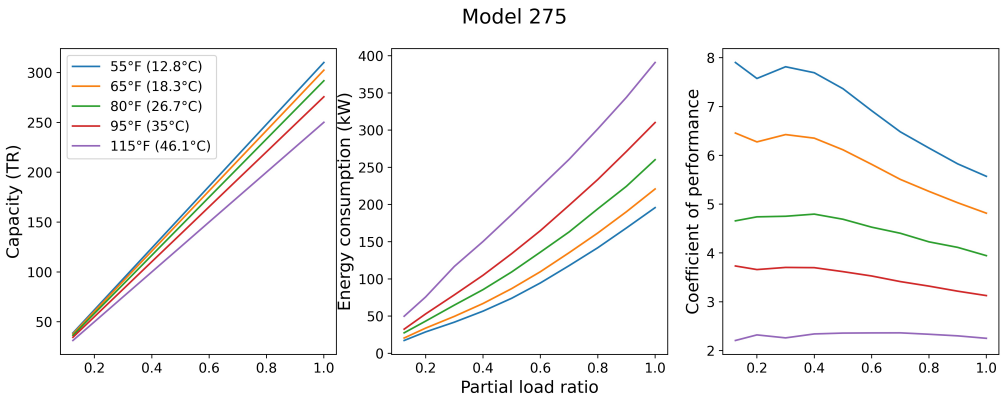

Figure B.6: Performance curves - Model 275

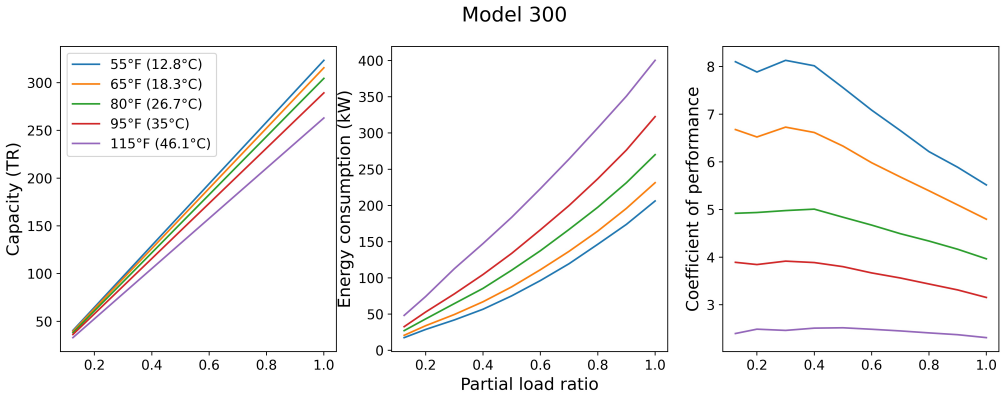

Figure B.7: Performance curves - Model 300

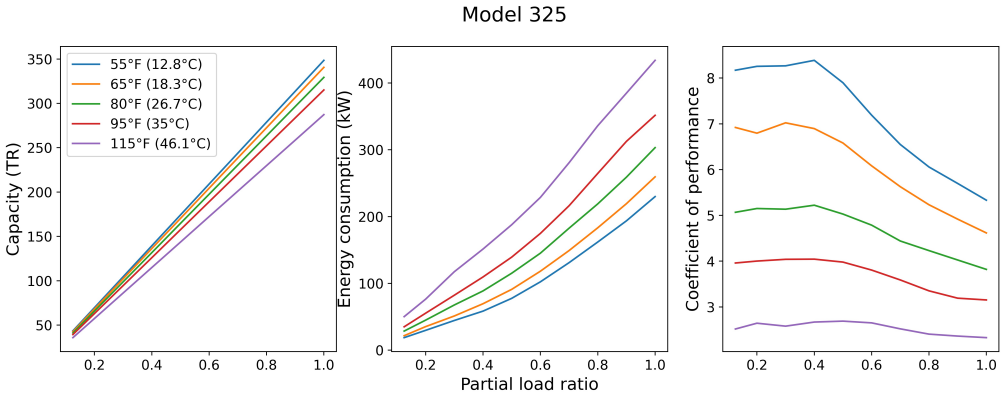

Figure B.8: Performance curves - Model 325

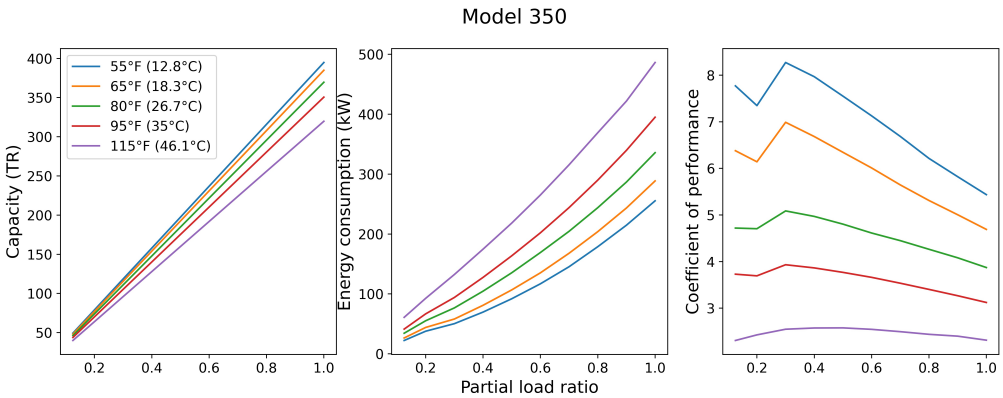

Figure B.9: Performance curves - Model 350

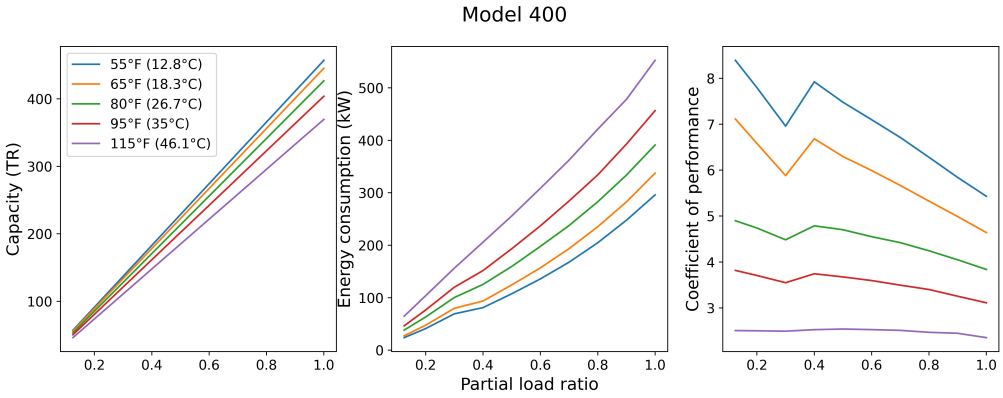

Figure B.10: Performance curves - Model 400

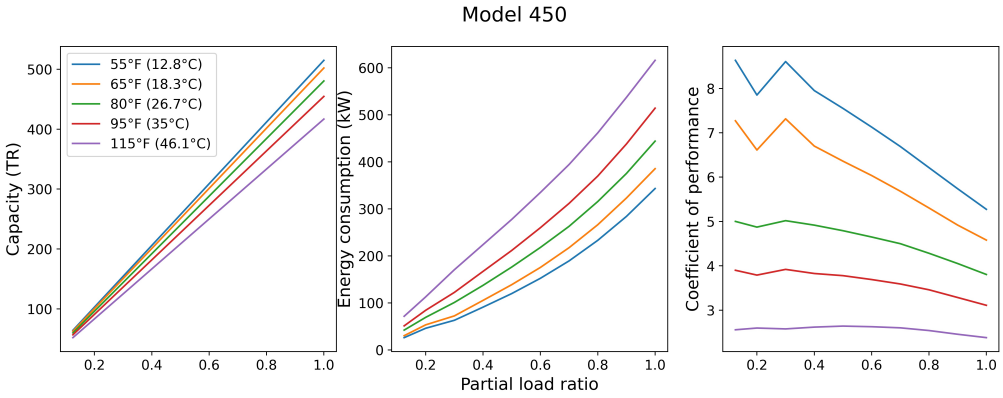

Figure B.11: Performance curves - Model 450

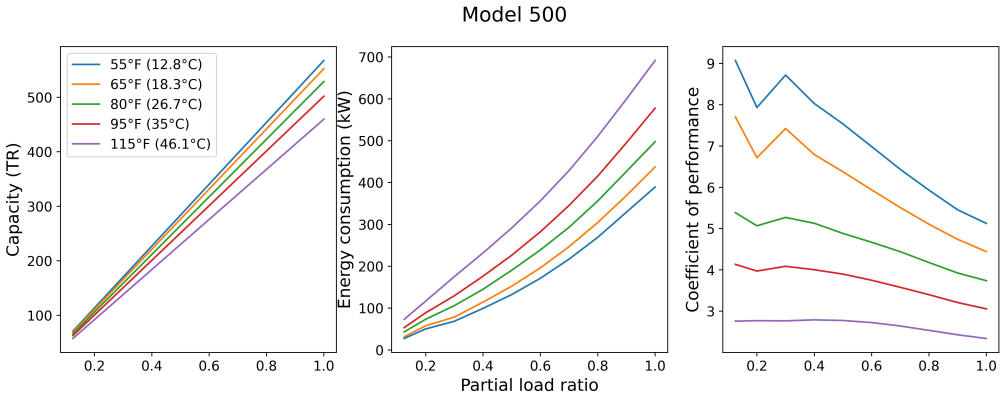

Figure B.12: Performance curves - Model 500